



Article

Investigation of the Mechanical Properties and Durability of Fiber-Reinforced Geopolymer Mortars Containing Metakaolin and Glass Powder

Mir Alimohammad Mirgozar Langaroudi ^{1,*}, Mohammad Mohtasham Moein ², Ashkan Saradar ³
and Moses Karakouzian ^{4,*}

¹ Department of Civil Engineering, Fouman and Shaft Branch, Islamic Azad University, Fouman 4351835875, Iran

² Department of Civil Engineering, Allameh Mohaddes Nouri University, Nour 4641859558, Iran; m.mohtasham.moein@gmail.com

³ Department of Civil Engineering, University of Guilan, Rasht 4199613776, Iran; saradar@msc.guilan.ac.ir

⁴ Department of Civil and Environmental Engineering and Construction, University of Nevada, Las Vegas, NV 89154, USA

* Correspondence: ali.mirgozar@iau.ac.ir (M.A.M.L.); mkar@unlv.nevada.edu (M.K.); Tel.: +98-911-140-0681 (M.A.M.L.); +1-702-895-0959 (M.K.)

Abstract: The increasing global emphasis on sustainable construction practices has spurred significant international research into developing durable and eco-friendly concrete materials. This study investigates the potential of metakaolin and glass powder as supplementary aluminosilicate materials in slag-based geopolymer mortars, aiming to enhance their mechanical properties and durability. To further improve the performance, polypropylene fibers were incorporated at various dosages. Therefore, 13 mixtures of geopolymer mortar based on blast furnace slag have been developed. The control mix does not contain fibers or slag replacement materials, whereas in the other formulations, glass powder and metakaolin have been employed as substitutes for slag at weight percentages (relative to the weight of slag) of 5% and 10%, separately and in combination. Additionally, the fiber-containing samples are divided into two groups based on the volume percentage of polypropylene fibers, comprising 0.2% and 0.4%. The results of the investigation show that the use of glass powder, particularly at a replacement percentage of 10%, leads to an improvement in the 28-day compressive strength. Furthermore, the mixes containing glass powder demonstrated higher flexural strength compared to those containing metakaolin, irrespective of the volume percentage of fibers. The best performance in the rapid chloride permeability test is associated with the mix containing a combination of glass powder and metakaolin at a replacement percentage of 10%. Satisfactory results have been obtained when using fibers at volume percentages of 0.2% and 0.4%. Additionally, this study utilized a fuzzy inference system to predict compressive strength. The results indicate that, by considering uncertainties, the compressive strength of the mortar can be predicted with an error of less than 1% without the need for complex mathematical calculations.

Keywords: geopolymer mortar; metakaolin; glass powder; polypropylene fibers; fuzzy logic



Academic Editors: Chris Goodier, Giuseppe Loprencipe and Valeria Vignali

Received: 28 October 2024

Revised: 4 January 2025

Accepted: 17 January 2025

Published: 21 January 2025

Citation: Mirgozar Langaroudi, M.A.; Mohtasham Moein, M.; Saradar, A.; Karakouzian, M. Investigation of the Mechanical Properties and Durability of Fiber-Reinforced Geopolymer Mortars Containing Metakaolin and Glass Powder. *Infrastructures* **2025**, *10*, 25.

<https://doi.org/10.3390/infrastructures10020025>

Copyright: © 2025 by the authors. Licensee MDPI, Basel, Switzerland. This article is an open access article distributed under the terms and conditions of the Creative Commons Attribution (CC BY) license (<https://creativecommons.org/licenses/by/4.0/>).

1. Introduction

The process of producing Portland cement has significant drawbacks [1–5]. Its production leads to the release of large amounts of carbon dioxide (CO₂) into the environment, with the production of one ton of Portland cement resulting in the emission of nearly one

ton of CO₂ [6–9]. Furthermore, climate change stemming from global warming has become one of the most serious environmental concerns worldwide [10–12]. The primary cause of global warming is the emission of greenhouse gases, and among these gases, CO₂ plays the most significant role, accounting for 65% of emissions [13–15]. Consequently, the Portland cement production process is recognized as one of the major sources of CO₂ emissions and global warming [16–18]. Experts estimate that the production of Portland cement accounts for 7% to 10% of global CO₂ emissions [19–21]. Therefore, finding an alternative to Portland cement is critical. In recent years, geopolymers have emerged as a new and environmentally friendly cementing agent, proposed as a substitute for Portland cement, which could lead to a reduction in the environmental issues associated with Portland cement production [22–26]. Geopolymer was first introduced in 1978 by Davidovits, a prominent French chemist, as a new class of binders belonging to the family of inorganic polymers [27]. Geopolymer concrete is characterized by the use of silica (Si) and alumina (Al)-rich aluminosilicate materials and an alkaline solution as the binding agent. The advantages of geopolymer concrete, in addition to its low energy production, include desirable mechanical properties and high durability in corrosive environments [28–31].

Geopolymer consists of two terms: (i) geo and (ii) polymer. The term ‘geo’ indicates geological or industrial materials (such as slag, fly ash, etc.), and modification of ‘polymer’ is also called a chain of molecules derived from macromolecules [32,33]. Figure 1a shows a schematic view of the geopolymer mortar/concrete creation process [34,35]. The two main pillars in the production of geopolymer mortar/concrete are the precursor (the result of agricultural/industrial waste) and the alkaline activator [34]. Geopolymerisation or alkali activation is a name that refers to the set of reactions between precursor (product of agricultural/industrial waste) and alkali sources (fly ash, slag, etc.) [35–37]. In this regard, Figure 1b presents a conceptual model of the geopolymerisation reaction based on Doxon et al. [38]. In the first stage (dissolution), the precursor and alkali activator are dissolved (amorphous components = aluminates and silicates). In the second stage, aluminates and silicates react with each other to finally produce aluminosilicate gel in the third stage. The resulting gel (Gel 1) is rich in aluminum because the reactive aluminum dissolves much faster than the silicon [35]. In the next step, when more silicon dissolves and participates in the process, the gel undergoes reorganization to form Gel 2 (zeolite precursor gel). Gel 2 is more stable than Gel 1 because Si-O bonds offer higher resistance than Al-O bonds [35]. Reorganization processes are carried out again to finally result in the formation of crystallized zeolite. Finally, similarly to OPC hydration, the gels coalesce and form a solid mass. Figure 1c reports some of the differences between conventional concrete/mortar and geopolymer [35]. Despite all the advantages of geopolymer elements, they have a downside as well; if alkalis are used excessively, efflorescence occurs, in which alkalis spread on the surface and react with CO₂, and finally, white carbonate develops [34,39]. Figure 1d schematically shows the efflorescence of geopolymers. Unfortunately, the great potential in using geopolymer concrete/mortar, which would lead to strides in sustainable development, is limited due to the lack of consistent guidelines [40]. However, some countries have provided standards for the use of these materials, which are (1) GB/T 29423 [41], (2) PAS 8820 (United Kingdom) [42], and (3) RSN 336-84 (Ukraine) [43].

Geopolymer concrete exhibits excellent resistance to chemical attacks, including acid, alkali, and sulfate attacks. This makes it ideal for applications in marine environments, industrial areas, and regions with aggressive soil conditions [44]. It also has demonstrated excellent resistance to chloride ion penetration, making it a promising material for use in harsh environments, particularly marine and coastal structures [45]. The dense microstructure of geopolymer concrete results in low permeability, reducing the ingress of water and chloride ions. This enhances the durability of the material in aggressive environments [46].

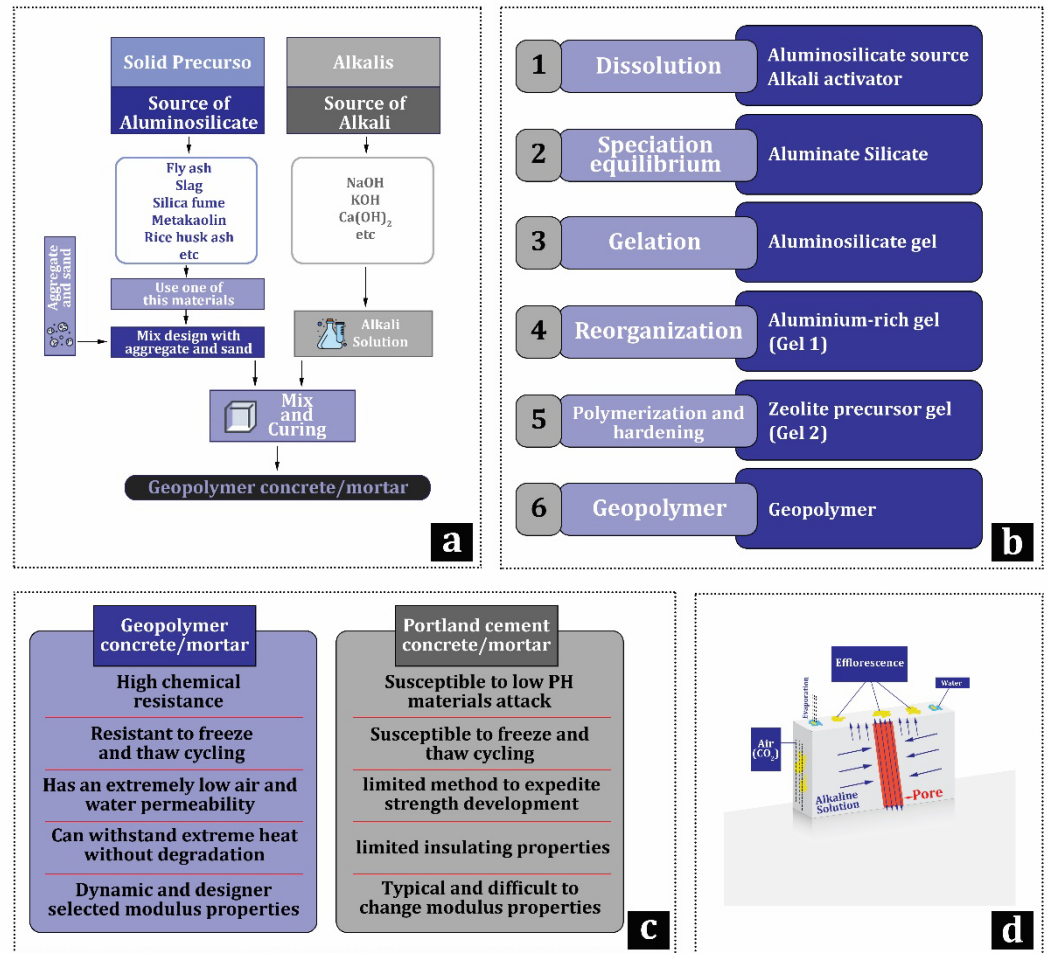


Figure 1. Geopolymer Mortar/Concrete: (a) Process of creation; (b) Conceptual model of geopolymerization; (c) Comparison with conventional concrete/mortar; (d) Efflorescence in geopolymer materials.

Geopolymeric materials, similarly to cementitious materials, exhibit weaknesses under tensile stresses and display brittle behavior. One effective strategy for enhancing ductility and transforming brittle behavior into ductile behavior is the incorporation of fibers into geopolymeric mixtures. The addition of fibers to concrete not only influences the improvement of the static resistance characteristics of the concrete but also significantly impacts the isotropy and homogeneity of the concrete body [47–55]. According to the definition by ACI 544, fiber-reinforced concrete is composed of hydraulic cement, fine or coarse aggregates, and discrete and discontinuous fibers. In fiber-reinforced concrete, pozzolans and other supplementary materials can be utilized similarly to conventional concrete [56]. In a laboratory study [57], the mechanical properties of glass fiber-reinforced geopolymer concrete based on fly ash were investigated, and sodium hydroxide (NaOH) and sodium silicate (Na₂SiO₃) were utilized as alkaline solutions (to activate the geopolymer reaction) at molar concentrations of 12, 16, and 20. Glass fibers were added to the geopolymer concrete in varying volumetric percentages from 0.1% to 0.5%. The concrete samples were cured under two conditions: one set was subjected to heat in an oven at 90 °C for 24 h, while the other set was cured in a natural environment. According to the results, the heat-cured samples exhibited better mechanical properties compared to the naturally cured ones. The heat-cured concrete sample, containing 0.3% glass fibers and a 16-molar sodium hydroxide, achieved a maximum compressive strength of 24.8 MPa after 28 days, whereas the naturally cured sample resulted in a strength of 22.2 MPa. A significant increase in

the tensile strength of the geopolymer concrete was observed due to the addition of glass fibers [57].

In another study [58], various durability tests on the impact of polypropylene fibers on geopolymer concrete were performed. The results indicate that the laboratory samples exhibited high compressive strength as well as extended longevity. For all mix proportions, particularly for mixtures containing up to 0.6% polypropylene fibers, the quality of the geopolymer concrete was assessed as excellent. Additionally, the results demonstrate that drying shrinkage in geopolymer concretes can be minimized by incorporating polypropylene fibers into the mix. The polypropylene fibers enhance the performance of geopolymer concrete by providing resistance to chloride penetration and increasing its lifespan [58]. In [59], the effects of three different proportions of basalt fibers on geopolymer mortars based on metakaolin produced with three types of aggregates were investigated. By adding 0%, 0.4%, 0.8%, and 1.2% basalt fibers for each group, a total of 12 different geopolymer mixes were obtained. According to the results, basalt fibers exhibited positive effects, particularly when used in a 0.8% to 1.2% range, leading to improvements of up to 25% in compressive strength and 50% in flexural strength [59]. Ruizhe et al. [60] experimentally investigated the impact of glass powder on the mechanical properties of metakaolin-based geopolymer concrete. The glass powder used in the preparation of the laboratory samples ranged from 0% to 20%. The results indicate that using low amounts of glass powder (5–10%) positively affects the samples' mechanical properties [60]. The compressive strength and microstructure of geopolymer concrete containing waste glass powder and fly ash were examined by Tawatchai et al. [61]. The results indicate that waste glass powder can be used as a substitute for fly ash in the production of geopolymer paste, achieving a 7-day compressive strength of 34–48 megapascals [61]. The damage caused by acidic environments to geopolymer mortars based on waste glass powder and calcium aluminate cement with moderate concentration was experimentally investigated by Vafaei et al. [62]. Their research findings demonstrate that the samples made with geopolymer cements exhibited better acid resistance compared to the reference samples [62].

In recent years, researchers have shown a growing interest in employing modern techniques such as artificial intelligence (AI) for the evaluation and prediction of the mechanical resistance of concrete [53,54,63–69], particularly geopolymer concrete, as an alternative to traditional statistical methods. Rathnayaka et al. [70] have provided a comprehensive review of machine learning methodologies utilized to predict the compressive strength of fly ash-based geopolymer concrete, a sustainable alternative to Ordinary Portland Cement. The authors categorized input parameters for model development based on feature selection and extraction and classify various machine learning approaches such as nonlinear regression, ensemble learning, and evolutionary programming. Their findings indicate the significance of hyperparameter adjustments on model performance and highlight existing gaps in the research. Their work aims to enhance the understanding of machine learning's role in optimizing geopolymer concrete design, providing insights for future investigations into sustainable, cement-free concrete solutions. Alaneme et al. [71] have explored the application of artificial intelligence in optimizing sustainable structural materials, particularly focusing on agro-waste-based green geopolymer concrete. The study involved a systematic literature review to assess AI techniques like FL, adaptive neuro-fuzzy inference systems (ANFIS), artificial neural networks (ANN), and gene expression programming (GEP), analyzing their methodologies and findings. Laboratory experiments were conducted to optimize aluminosilicate precursors and alkaline activators. The findings highlight the advantages and challenges of AI in improving geopolymer-concrete production, emphasizing its potential to enhance mix design, curing conditions, and material selection while minimizing environmental impacts. Wang et al. [72] have explored the use of AI to predict

the compressive strength of geopolymer concrete as a sustainable alternative to ordinary Portland cement. The study employed various AI techniques, including ANN, ANFIS, and GEP, to develop predictive models. Statistical parameters assessed model performance, while sensitivity and parametric analyses were conducted on input variables. The findings indicated that GEP outperforms other methods in accurately predicting the compressive strength of fly ash and ground granulated blast furnace slag-based GP concrete. Dao et al. [73] have investigated the use of hybrid AI methods to predict the compressive strength of geopolymer concrete made with 100% waste slag aggregates. They introduce two models: a particle swarm optimization-based adaptive network-based fuzzy inference system (PSOANFIS) and a genetic algorithm-based adaptive network-based fuzzy inference system (GAANFIS). Using 21 different mixes and 210 specimens, the study varied parameters like sodium hydroxide concentration and mixing ratios to assess compressive strength. The results indicate that both models effectively predict strength, with PSOANFIS slightly outperforming GAANFIS. This research offers a faster, more cost-effective approach to optimizing GPC formulations.

Ali et al. [74] have conducted a systematic literature review on the utilization of machine learning (ML) and deep learning (DL) techniques to predict the properties of eco-friendly concrete alternatives, including self-compacting concrete and geopolymer concrete. The study analyzed various predictive models such as ANN, support vector machines (SVM), and boosting methods. The findings reveal that ANNs are particularly effective for geopolymer concrete, while bagging and boosting methods perform well in predicting self-compacting concrete properties. The review highlights AI's significant potential to optimize concrete mix designs, enhance sustainability in the construction industry, and reduce the need for costly experimental testing, while also identifying key challenges and gaps for future research. Krishna and Rao [75] investigated the potential of geopolymer concrete as a sustainable alternative to traditional cement-based concrete, which has significant environmental impacts. They focused on predicting the strength and durability of geopolymer concrete based on molar concentration of the binder using fuzzy logic (FL). The study demonstrated that accurate strength predictions can be achieved through the analysis of molar concentration data. The findings highlight the viability of using FL to assess the mechanical properties of geopolymer concrete, paving the way for more eco-friendly construction materials. Terrones-Saeta et al. [76] investigated the potential of geopolymers made from biomass bottom ashes and brick dust as a sustainable alternative to traditional ceramics in the building materials industry. The study involved creating various test samples with different proportions of these waste materials and analyzing their physical and mechanical properties. FL and data mining techniques were employed to explore the relationships between these properties and the compressive strength of the geopolymers. The findings demonstrate that geopolymers can be effectively produced using these waste materials, achieving acceptable properties for replacing conventional ceramics.

2. Research Framework and Significance

The construction industry has increasingly moved towards sustainable development in recent years, paying greater attention to reducing environmental impacts. Reports [1,77] indicate that a significant portion of greenhouse gas emissions, particularly CO₂, are associated with the construction sector. In this context, the cement production process, recognized as one of the major polluters, significantly contributes to CO₂ emissions. Given the substantial share of CO₂ in greenhouse gases emissions produced by various countries, it is essential to seek sustainable alternatives and materials such as geopolymer mortars that can mitigate negative environmental effects. This study examines geopolymer mortars containing glass powder, metakaolin, and polypropylene fibers, analyzing various experi-

mental results, including compressive strength, flexural strength, electrical resistivity, water absorption, and chloride ion penetration resistance. Additionally, the use of FL to predict the compressive strength of geopolymer mortars in this research presents an innovative and efficient approach for evaluating these materials' performance.

Moreover, this research holds particular significance considering the lack of studies on the examination of geopolymer mortars in chloride environments. The development and utilization of such mortars in various structures can enhance durability and sustainability in corrosion-prone environments. Structures such as bridges, coastal constructions, and marine infrastructure, which are exposed to chloride conditions, can greatly benefit from the findings of this study. Overall, the objective of this research is to provide innovative and sustainable solutions that meet the growing demands of the construction industry and contribute to achieving sustainable development goals. An illustrative flowchart is provided to represent the structure of the methodology and the interconnections between different aspects of the research (Figure 2). This comprehensive approach facilitates a thorough understanding of the behavior and performance of geopolymer mortars in varying conditions.

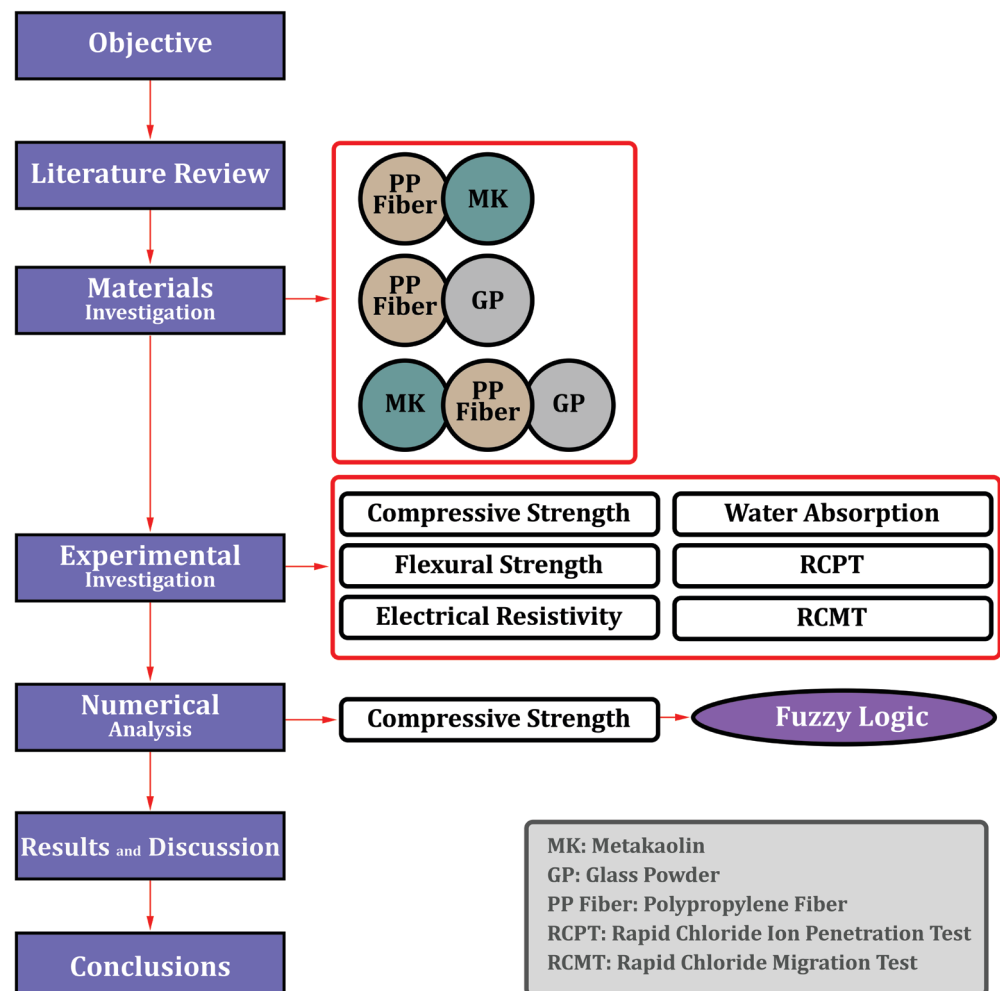


Figure 2. Methodology.

3. Experimental Program

3.1. Materials and Mix Proportions

To achieve the objectives of this research, 13 mix designs of geopolymer mortars based on blast furnace slag have been developed. The slag used was sourced from the Isfahan

Steel Company in Esfahan, Iran and has a specific weight of 2410 kg/m³. The chemical composition of the slag is presented in Table 1. The control mix does not contain fibers or any substitute for slag, while in the other mix designs, glass powder and metakaolin have been used as substitutes for slag at weight percentages (relative to the weight of the slag) of 5% and 10%, individually and in combination. The chemical analysis of the metakaolin used is also presented in Table 1. The fiber-containing mixtures were divided into two groups based on the volumetric percentage of polypropylene fibers: 0.2% and 0.4%. The fibers utilized have a length of 12 mm, a density of 910 kg/m³, and a tensile strength of 35 MPa. In the present study, slag was utilized as a source of aluminosilicate for the production of geopolymer mortar. In the control sample, 700 kg/m³ of slag was used, while in the other samples, a portion of the slag (with varying weight percentages) was replaced with glass powder and metakaolin. The activation of the alkaline base material (slag) was facilitated using sodium hydroxide and sodium silicate as the alkaline activating solution. Caustic soda (sodium hydroxide, NaOH) was mixed with water in powder form at a molarity concentration of 10 for the preparation of geopolymer mortar samples. Furthermore, a water glass solution (sodium silicate, Na₂SiO₃) with a density of 1250 kg/m³ was utilized. The ratio of the alkaline silicate solution to the geopolymeric aluminosilicates for all samples was maintained at 0.5 by weight.

Table 1. Chemical composition of the used blast furnace slag, metakaolin, and glass powder.

Chemical Analysis	Slag	Metakaolin	Glass Powder
SiO ₂	37.21	51.52	70.02
Al ₂ O ₃	11.56	40.18	3.52
Fe ₂ O ₃	1.01	1.23	1.65
CaO	36.75	2	10.41
MgO	8.25	0.12	1.32
SO ₃	0.97	0	0.08
Na ₂ O	0.61	0.08	11.18
K ₂ O	0.7	0.53	0.89
MnO	0.99	0	0
TiO ₂	1.23	2.27	0.1
L.O.I	0.02	2.01	0.78

To achieve optimal fluidity and facilitate improved particle distribution within the mortar mixture, a polycarboxylate ether-based superplasticizer, marketed under the trade name FARCO PLAST P10N and manufactured by the Shimi Sakhteman Company (Tehran, Iran), has been employed. The specifications of the superplasticizer used are reported in Table 2. To ensure consistent workability across all mixture designs, the flow value of the geopolymer mortar was maintained at a constant value of 105 ± 5%. The flow value was measured using a flow table in accordance with ASTM C1437. The sand employed in this study is a river-rounded type. The saturated surface-dry bulk density of the sand is 2611 kg/m³ with a water absorption of 2.4%. The gradation of the sand conforms to ASTM C33 [78], as illustrated in Figure 3. Detailed mix designs are presented in Table 3.

Table 2. Specifications of superplasticizer.

Technical Features	
Generation	3
Physical state	Liquid
Color	Opaque green
Specific weight	1.2 ± 0.02 kg/lit

Table 2. Cont.

Technical Features	
Chlorides (PPM)	500 max.
Chemical base	Modified polycarboxylate ether

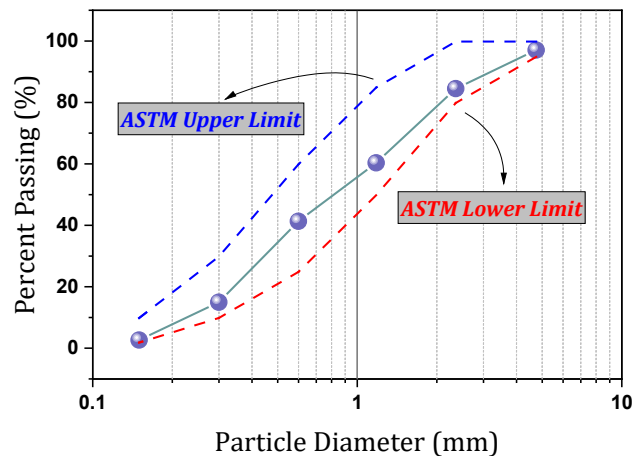


Figure 3. Granulation curve of used sand.

Table 3. Mix proportions of geopolymer mortar.

N.O.	Mix Code	Slag	Metakaolin	Glass Powder	PP Fiber	Na ₂ SiO ₃	NaOH	Sand	SP
		Kg/m ³	%	%	%	Kg/m ³	Kg/m ³	Kg/m ³	Kg/m ³
1	Control	700	0	0	0	250	100	1191	1.633
2	M5P2	665	5	0	0.2	250	100	1191	1.100
3	M10P2	630	10	0	0.2	250	100	1191	1.433
4	G5P2	665	0	5	0.2	250	100	1191	1.333
5	G10P2	630	0	10	0.2	250	100	1191	1.567
6	M2.5G2.5P2	665	2.5	2.5	0.2	250	100	1191	1.167
7	M5G5P2	630	5	5	0.2	250	100	1191	2.400
8	M5P4	665	5	0	0.4	250	100	1191	1.833
9	M10P4	630	10	0	0.4	250	100	1191	1.233
10	G5P4	665	0	5	0.4	250	100	1191	1.400
11	G10P4	630	0	10	0.4	250	100	1191	2.400
12	M2.5G2.5P4	665	2.5	2.5	0.4	250	100	1191	1.767
13	M5G5P4	630	5	5	0.4	250	100	1191	2.667

In the naming convention of the mix designs, ‘ctrl’ denotes the control mix, while ‘G’ and ‘M’ represent glass powder and metakaolin, respectively. The numbers following these letters indicate the percentage replacement of these materials with slag. Additionally, the letter ‘P’ denotes polypropylene fibers. After demolding, the specimens were cured in a water tank at a temperature of 23 ± 2 °C until testing.

3.2. Tests

This study comprises five tests: (i) compressive strength, (ii) flexural strength, (iii) electrical resistivity, (iv) water absorption, and (v) rapid chloride ion migration. Table 4 presents the specifications and details of the tests conducted in this study.

- The compressive strength was tested according to ASTM C-109 [79] on cubic specimens measuring $50 \times 50 \times 50$ mm at the ages of 7 and 28 days.
- The flexural test was conducted using the three-point method in accordance with ASTM C348 [80] after curing for 28 days. In this test, prism specimens measuring $160 \times 40 \times 40$ mm were utilized.
- Electrical resistivity, as one of the characteristics of mortar and concrete, indicates certain important properties, including permeability and, consequently, water absorption. The higher the electrical resistivity, the lower the permeability. This test was performed according to ASTM C1760 [81], but was conducted on cubic specimens (measuring $50 \times 50 \times 50$ mm) after curing the samples for 28 days. While cylindrical specimens are preferred for standardized testing according to ASTM C1760, the use of cubes is not uncommon in the scientific literature, especially in studies where direct comparison with other properties obtained from cube specimens is desired. Figure 4 shows the experimental setup for measuring electrical resistivity used in this study.

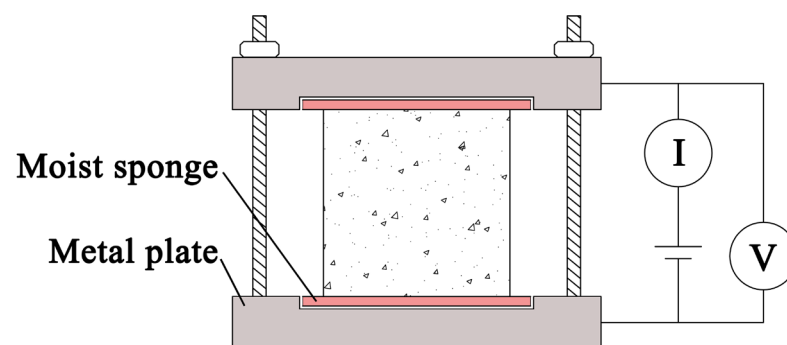
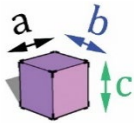
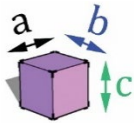
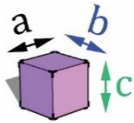
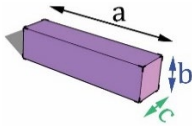
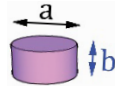


Figure 4. The experimental setup for measuring electrical resistivity.

- The final water absorption test was conducted according to ASTM C-642 [82] at 28 days on cubic specimens measuring $50 \times 50 \times 50$ mm.
- The Rapid Chloride Migration Test (RCMT) accelerates the penetration of chloride ions into cementitious composites by applying an electric potential across the ends of the mortar or concrete specimen. Subsequently, the specimen is broken, and the depth of chloride ion penetration is visually observed and measured to calculate the chloride ion diffusion coefficient. The RCMT is conducted according to the NT BUILD 492 standard [83]. This test was performed on specimens with a diameter of 100 mm and a height of 50 mm after curing for 28 days. The arrangement of the specimens in the experimental setup is depicted in Figure 5. This test simulates an unsteady state and evaluates the resistance of cementitious composites to chloride penetration.

Table 4. The specifications and details of the tests.

N.O.	Test	Standard	Curing	Dimension (cm)			Number of Samples	Shape	
				a	b	c			
1	CS	ASTM C-109 [79]	7 and 28	5	5	5	78	Cube	
2	ER	ASTM C-1760 [81]	28	5	5	5	39	Cube	
3	WA	ASTM C-642 [82]	28	5	5	5	39	Cube	
2	FS	ASTM C-348 [80]	28	16	4	4	39	Prism	
3	RCMT	NT BUILD 492 [83]	28	10	50	---	39	Cylinder	

CS = Compressive Strength, ER = Electrical Resistivity, WA = Water absorption, FS = Flexural Strength.



Figure 5. Rapid Chloride Migration Test (RCMT).

4. Prediction Model—Fuzzy Logic (FL)

Fuzzy set theory was first introduced by Professor Lotfi A. Zadeh in 1965 [1,84]. Then, in the early 1970s, the first applications of this theory were presented in engineering sciences with the emergence of FL. Since then, we have witnessed the rapid growth of both theoretical and practical aspects of fuzzy set theory by scientists from various disciplines. Today, this theory is applied in almost all areas of industry and academia [1]. The most significant advantage of FL compared to classical logic is its ability to represent human knowledge and experience in mathematical terms. This enables us to effectively model real-world problems. Fuzzy Inference Systems (FIS) are built upon “if-then” rules, allowing for the establishment of relationships between multiple input and output variables [1]. Consequently, FIS can be employed as a predictive model for scenarios involving high levels of uncertainty in input and output data, as classical prediction methods such as regression often struggle to adequately account for such uncertainties. FIS are developed using fuzzy implication operators and fuzzy relation compositions [85]. Numerous studies have successfully employed FIS to investigate concrete and mortar and to predict the

outcomes of experiments [85]. A minimum-maximum FIS was employed in this study. The center of gravity method was utilized for defuzzification. Furthermore, the Mamdani fuzzy implication method was adopted. Table 5 presents the range of input and output values along with their corresponding linguistic grading. Figure 6 illustrates the membership functions of the input and output variables used in the fuzzy system.

Table 5. Range of input and output values and corresponding linguistic gradation.

Input	Fuzzy MF	Range
Slag [kg/m ³]	Low	0–661
	Medium	650–690
	High	680–700
Metakaolin [%]	Low	0–3
	Medium	1.5–4.5
	High	4–8
	Very High	6–10
Glass powder [%]	Low	0–3
	Medium	1.5–4.5
	High	4–8
	Very High	6–10
Polypropylene fiber [%]	Low	0–0.15
	Medium	0.1–0.3
	High	0.25–0.4
Superplasticizer [kg/m ³]	Low	1.1–1.7
	Medium	1.6–2.2
	High	2–2.667
Output	Fuzzy MF	Range
Compressive strength [Mpa]—7 days	Very Low	55.63–60
	Low	58–64
	Medium	62.04–68
	High	65–70
	Very High	69–72.39
Compressive strength [Mpa]—28 days	Very Low	75.37–78
	Low	77.18–80.50
	Medium	79.04–82.46
	High	82–85
	Very High	84–86.84

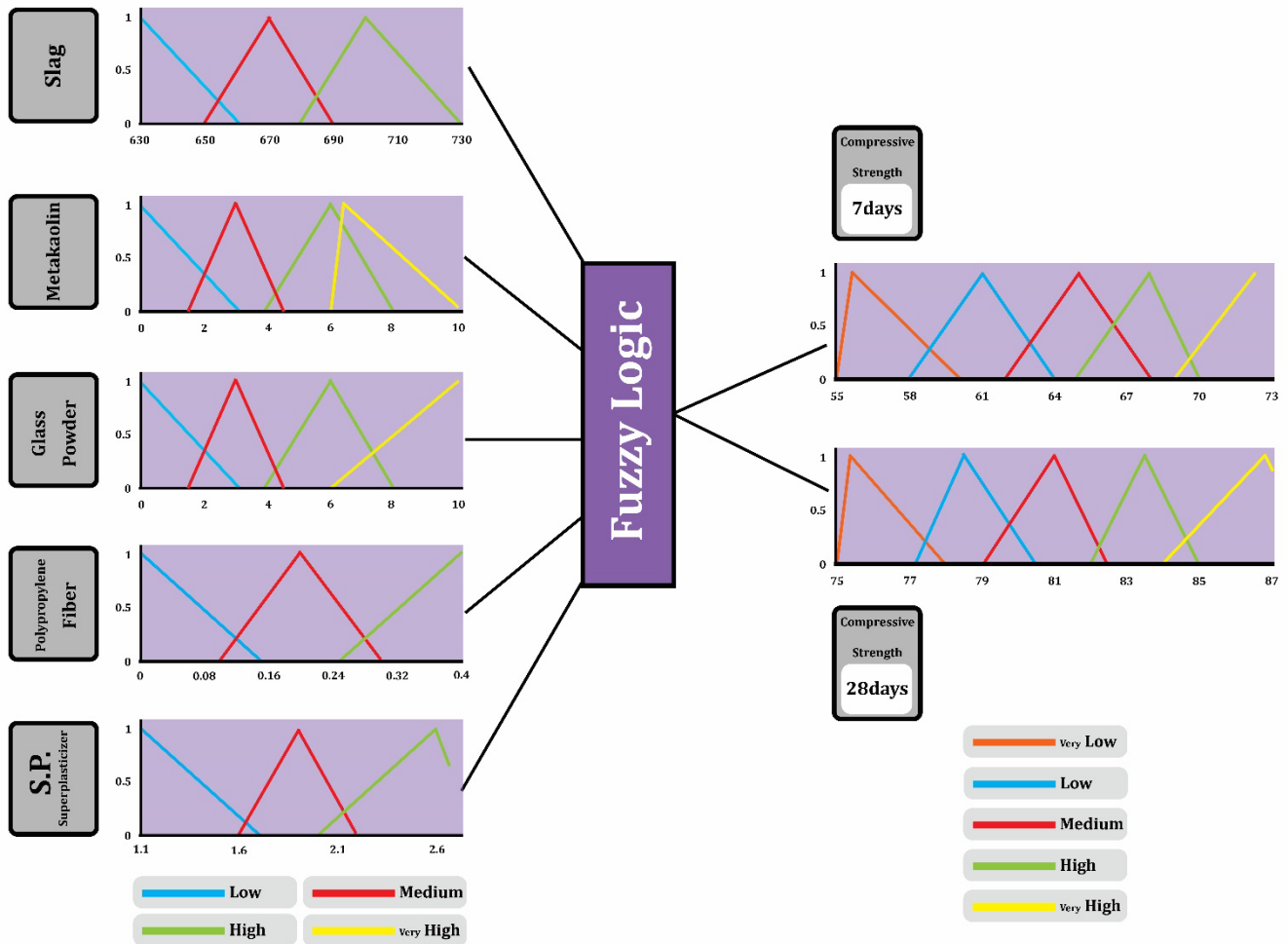


Figure 6. Inputs and outputs in the FL model.

5. Results and Discussion

5.1. Compressive Strength

Compressive strength is a fundamental property that underpins the mechanical performance of mortars and concretes. In this study, compressive strength was evaluated at both early age (7 days) and at 28 days.

5.1.1. Early Compressive Strength (7-Day)

Figure 7 illustrates the results of compressive strength at 7 and 28 days. The changes (decreases/increases) in the compressive strength of the geopolymer mortar mixtures relative to the control mixture are reported in Figure 8. The compressive strength for the control mixture was found to be 63.412 MPa (Figure 7a). Based on the obtained results, substituting a portion of slag with weight percentages of 5% and 10% of metakaolin in both groups containing 0.2% and 0.4% fibers (M5P2, M10P2, M5P4, and M10P4) resulted in a decline in compressive strength compared to the control sample. Notably, as the percentage of metakaolin substitution increased, the degree of strength reduction also increased. In this regard, the recorded reductions in strength for mixtures M5P2, M10P2, M5P4, and M10P4 were 0.978%, 0.398%, 5.716%, and 10.194%, respectively. On the other hand, the incorporation of glass powder led to an increase in compressive strength. The analysis of mixtures G5P2 and G10P2 demonstrates an increase in compressive strength of 5.268% and 4.807%, respectively, at early ages, while mixtures G5P4 and G10P4 exhibited increases of 5.154% and 14.168%, respectively. The enhancement in strength caused by increasing the glass

powder content in the mixture was observed by other researchers [60,61]. In the hybrid mixtures (containing metakaolin, glass powder, and polypropylene fibers), the analysis of the mixture M2.5G2.5P2 indicated an increase in compressive strength of 7.854%. However, increasing the substitution percentage of polypropylene fibers to 0.4% (M2.5G2.5P4) disrupted the performance of the matrix, resulting in a reduction of approximately 12% in compressive strength. The investigation of hybrid mixtures M5G5P2 and M5G5P4 revealed improvements in compressive strength of 2.94% and 1.054%, respectively.

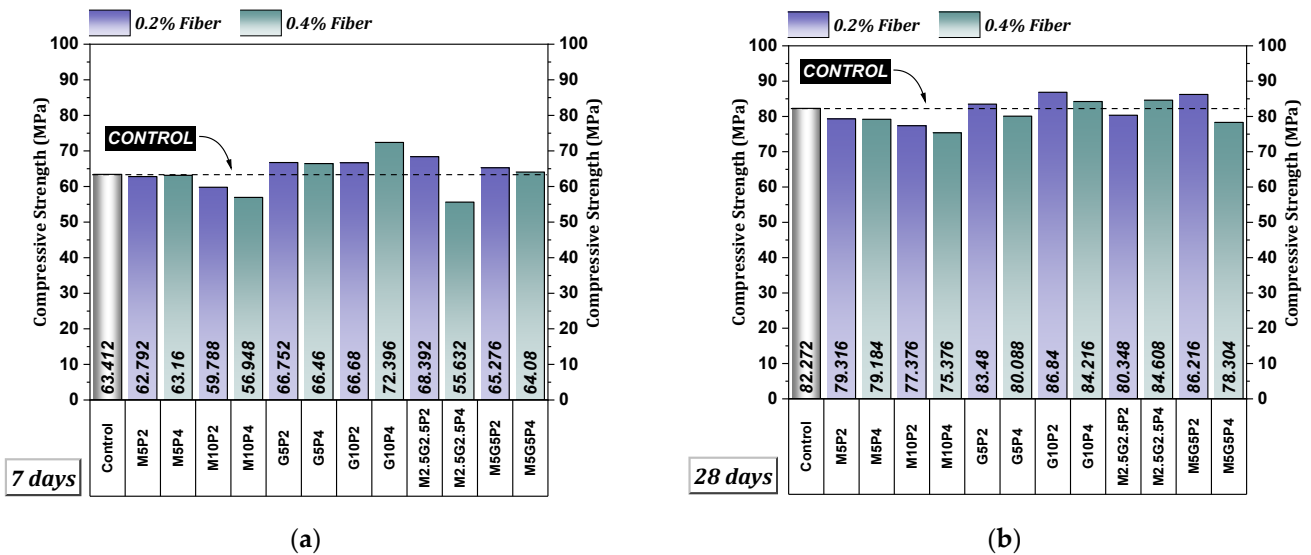


Figure 7. Compressive strength results: (a) 7 days; (b) 28 days.

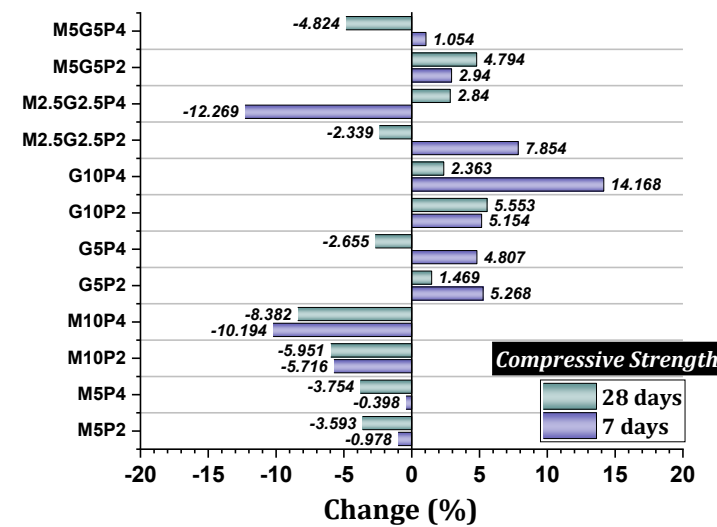


Figure 8. Changes in compressive strength at 7 and 28 days.

5.1.2. Standard Compressive Strength (28-Day)

According to Figure 7b, the 28-day compressive strength for the control mixture was recorded at 82.272 MPa. Similarly to the 7-day compressive strength, the presence of metakaolin in the mixture weakened the structure of the geopolymer mortar such that the increase in the percentage of metakaolin substitution from 5% to 10% resulted in a more rapid decline in compressive strength (Figure 8). In this regard, the analysis of mixtures M5P2, M10P2, M5P4, and M10P4 showed reductions in strength of 3.593%, 3.754%, 5.951%, and 8.382%, respectively. The mixtures containing metakaolin consistently exhibited lower

compressive strength than the control mixture with increasing curing age. This may be due to increased metakaolin content consuming more alkali activators, leading to a reduced amount of alkali available for the geopolymerization reaction. A similar trend was observed by Mohamed Amin et al. [86]. The use of glass powder in the geopolymer mixture at a level of 5% combined with 0.2% polypropylene fibers (G5P2) increased in 28-day compressive strength of 1.482%. This could be due to an improvement in microstructure caused by the filler effect of glass powder. Glass powder can also act as nucleation sites for the growth of geopolymer gel, leading to a more refined microstructure with smaller pores. Conversely, when the amount of polypropylene fibers was increased to 0.4% (G5P4), a reduction in compressive strength of 2.655% was observed. More fiber content can disrupt the formation of the geopolymer matrix by interfering with the reaction between the alkaline activator and the source materials. When glass powder was substituted at a level of 10% in the mixtures, the results for G10P2 and G10P4 showed improvements in compressive strength of 5.553% and 2.363%, respectively. This may be related to the stronger bonding between fibers and the matrix, which is caused by enhancing the matrix by incorporating glass powder [87]. The analysis of hybrid mixtures (containing metakaolin, glass powder, and polypropylene fibers) indicated an increase in compressive strength of 2.339% for the mixture M2.5G2.5P2, while a decrease in compressive strength of 2.384% was observed for the mixture M2.5G2.5P4. This suggests that when metakaolin and glass powder were present at a level of 2.5%, the inclusion of 0.4% polypropylene fibers yielded a more optimal result; however, for the combination of metakaolin and glass powder at 5%, the results were reversed. In this context, the examination of the mixture M5G5P2 revealed an increase in compressive strength of 4.794%, while the analysis of the mixture M5G5P4 indicated a decrease in compressive strength of 4.824%.

5.2. Flexural Strength—28 Days

Figure 9a displays the flexural strength results of the geopolymer mixtures at 28 days of curing. Additionally, Figure 9b illustrates the changes in the flexural strength of the mixtures in comparison to the control mixture. The flexural strength for the control mixture was determined to be 12.01 MPa. The results of the flexural strength test on the geopolymer mortar indicate that the combination of polypropylene fibers and metakaolin powder has a positive effect on its flexural strength. This could be attributed to the improved microstructure resulting from the incorporation of metakaolin and the fiber reinforcement effect of the polypropylene fibers. Similar findings were reported in previous studies [88]. The mixture M5P2 (5% metakaolin and 0.2% fibers) exhibited the best performance with an 8.774% increase in flexural strength, while the mixture M5P4 (5% metakaolin and 0.4% fibers) showed only a 6.001% increase, indicating the potential for interference in the mortar matrix with an increase in fiber content. The mixture M10P2 (10% metakaolin and 0.2% fibers) demonstrated only a 4.585% improvement in flexural strength, and M10P4 (10% metakaolin and 0.4% fibers) achieved a 5.751% increase, making it a successful combination for optimizing flexural strength. These results indicate that the appropriate and correct ratios of polypropylene fibers and metakaolin can lead to enhanced mechanical properties. The examination of mixtures containing polypropylene fibers and glass powder also indicates that these materials have a positive effect on flexural strength. The mixture G10P2 (10% glass powder and 0.2% polypropylene fibers) displayed the highest flexural strength with a 17.487% increase, likely due to the high reinforcing properties of glass powder and its synergistic effect with polypropylene fibers, as this combination facilitates more effective energy absorption and load distribution. Meanwhile, the mixture G5P2 (5% glass powder and 0.2% fibers) showed a 12.568% increase, and G5P4 (5% glass powder and 0.4% fibers) exhibited a 10.747% increase, respectively, achieving acceptable performance.

However, it is evident that increasing the percentage of glass powder and using a lower percentage of fibers compared to the mixture G10P4 had a greater impact on flexural strength. These results suggest that the optimal ratio of glass powder and fibers can play a key role in enhancing the mechanical properties of concrete [60,61,89].

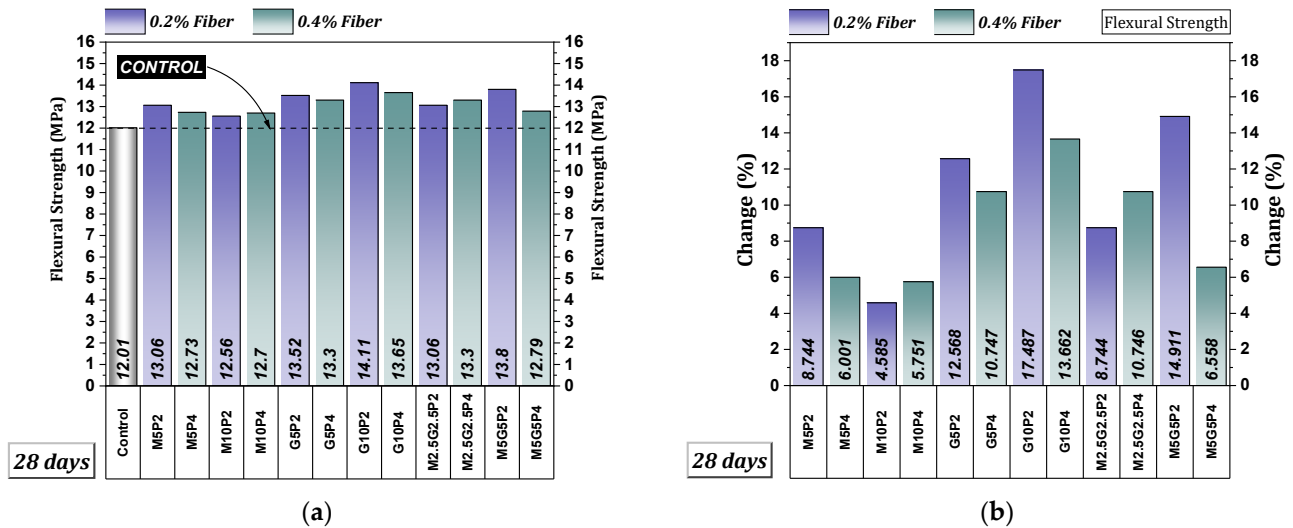


Figure 9. (a) Flexural strength results. (b) Flexural strength changes.

Furthermore, the results indicate that increasing the percentage of glass powder and metakaolin, along with polypropylene fibers, generally leads to an enhancement in the flexural strength of geopolymer mortar. The findings reveal that, as the percentage of polypropylene fibers increases, particularly from 0.2% to 0.4%, the flexural strength significantly increases as observed in the mixture M2.5G2.5P4, which exhibited a 10.746% increase compared to the mixture M2.5G2.5P2, which showed an 8.744% increase. The mixture M5G5P2 (containing 5% glass powder, 5% metakaolin, and 0.2% fibers) demonstrated the best performance with a 14.911% increase. This improvement may be attributed to enhanced bonding between the different components and better stress distribution [88,90]. Conversely, the mixture M5G5P4 (5% glass powder, 5% metakaolin, and 0.4% fibers) showed a 6.658% increase, indicating a potential negative effect of increased fiber percentage on flexural strength, which may be due to interference between the fibers and the mortar structure, thereby reducing cohesion within the mortar matrix. Therefore, maintaining an appropriate balance between the components is essential to achieve maximum flexural strength [88].

5.3. Electrical Resistivity—28 Days

Figure 10a illustrates the electrical resistivity results of the 28-day geopolymer mixtures. Additionally, Figure 10b reports the changes in electrical resistivity of the geopolymer mixtures compared to the control mixture. The 28-day electrical resistivity for the control mixture was 9.68 KΩ·cm. The results of the electrical resistivity indicate that the ratio of metakaolin to polypropylene fibers has a significant impact on the electrical resistivity of geopolymer mortar. Specifically, the M5P2 sample, which contains 5% metakaolin and 0.2% polypropylene fibers, demonstrates a 9.505% increase in electrical resistivity. This increase may be attributed to the improved dispersion of metakaolin particles and the enhancement of interconnections between them, leading to reduced permeability and better distribution of electrical charge [91]. Conversely, an increase in polypropylene fiber content to 0.4% in the M5P4 mixture results in a 3.203% decrease in electrical resistivity, which may be due to increased porosity caused by the fiber’s introduction. Furthermore, increasing the

metakaolin percentage to 10% in the M10P2 and M10P4 mixtures has a positive effect on electrical resistivity, indicating that the quality of metakaolin has a more dominant influence on the electrical properties of mortar compared to the content of polypropylene fibers [91]. Overall, the results suggest that optimizing the combination of polypropylene fibers and metakaolin can lead to improved electrical performance of geopolymer mortars.

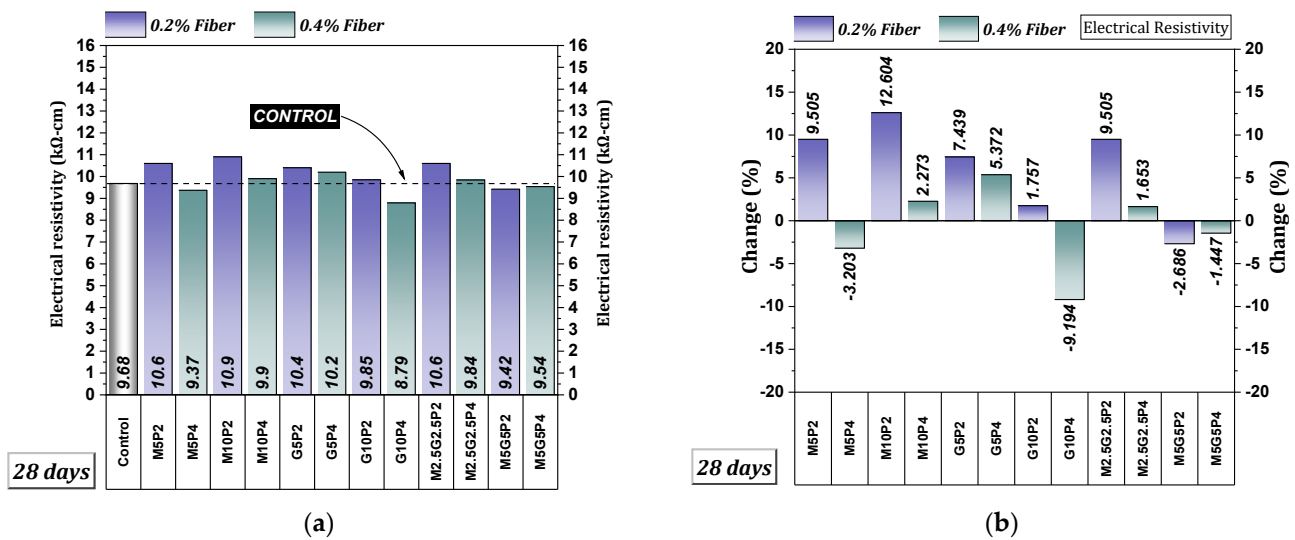


Figure 10. (a) Electrical resistivity results. (b) Electrical resistivity changes.

Based on the electrical resistivity results of geopolymer mortar samples containing glass powder and polypropylene fibers, the combination of these two materials has a significant impact on the electrical resistivity of the mortar. The G5P2 mixture, which contains 5% glass powder and 0.2% polypropylene fibers, exhibits a 7.439% increase in electrical resistance. This increase may be attributed to improvements in the microstructure of the mortar due to the glass powder, which contributes to increased density and reduced permeability, thereby enhancing electrical resistivity [60]. Furthermore, in the G5P4 mixture, with an increased fiber content of 0.4% while maintaining 5% glass powder, a 5.372% increase in electrical resistivity is observed, indicating that fibers also contribute to strengthening electrical resistivity in this composition. However, in the G10P4 mixture, where the glass powder percentage is increased to 10% and fibers are maintained at 0.4%, a decrease of 9.194% in electrical resistance occurs. This may be due to an imbalance in the ratios of glass powder to fibers, ultimately leading to structural weakness and reduced electrical resistance. Thus, it appears that excessive amounts of glass powder may negatively affect the stress and positive charge distribution within the composite, while the combination of fibers and glass powder can enhance the electrical resistivity of the mortar at appropriate levels.

The results of the electrical resistivity tests on geopolymer mortar samples composed of polypropylene fibers, glass powder, and metakaolin indicate that a precise balance among these materials can have a significant impact on the electrical resistance of the mortar. Specifically, the M2.5G2.5P2 mixture, which contains 2.5% glass powder, 2.5% metakaolin, and 0.2% polypropylene fibers, demonstrates a 9.505% increase in electrical resistivity. This increase may be attributed to the formation of an optimal structure and mechanical and chemical synergy between metakaolin and glass powder, leading to improved microscopic properties and reduced permeability in the matrix [92]. Additionally, in the M2.5G2.5P4 mixture with an increased fiber content of 0.4%, a continued rise in electrical resistance (1.653%) is observed; however, this increase is less pronounced compared to the previous mix (M2.5G2.5P2) due to several influencing factors. Conversely, in the M5G5P2 and

M5G5P4 mixtures, where the percentages of glass powder and metakaolin are increased to 5%, a decrease in electrical resistivity of 2.686% and 1.447% is observed, respectively. This decline may result from the saturation of the mortar with higher contents of glass powder and metakaolin, which can lead to the formation of networks that are imbalanced and exhibit poor electrical conductivity. Therefore, it seems that the optimal ratios of these materials are critical, and failing to maintain these ratios could result in a reduction in the mortar’s functional properties.

5.4. Final Water Absorption—28 Days

Figure 11a presents the final water absorption results of the geopolymer mixtures. Additionally, Figure 11b reports the changes in water absorption relative to the control mixture. The water absorption value for the control mixture was found to be 3.97%. The results of water absorption for geopolymer mortar samples indicate that variations in the dosage of metakaolin and polypropylene fibers have a significant impact on this property. For the M5P2 mixture, which contains 5% metakaolin and 0.2% polypropylene fibers, a reduction in water absorption of 11.839% was observed, likely due to improvements in the microstructure of the mortar and increased matrix adhesion. Conversely, in the M5P4 mixture, where the polypropylene fiber content was increased to 0.4% while maintaining 5% metakaolin, water absorption increased by 2.016%. This increase may be attributed to the presence of an additional fibrous structure, which creates more voids and potentially enhances the water absorption force [58]. Furthermore, in the M10P2 and M10P4 mixtures, an increase in the percentage of metakaolin to 10%, alongside polypropylene fibers, led to reductions in water absorption of 9.824% and 3.779%, respectively. This decrease may be due to the formation of a denser and stronger structure resulting from metakaolin, which enhances the water-repellent properties [93].

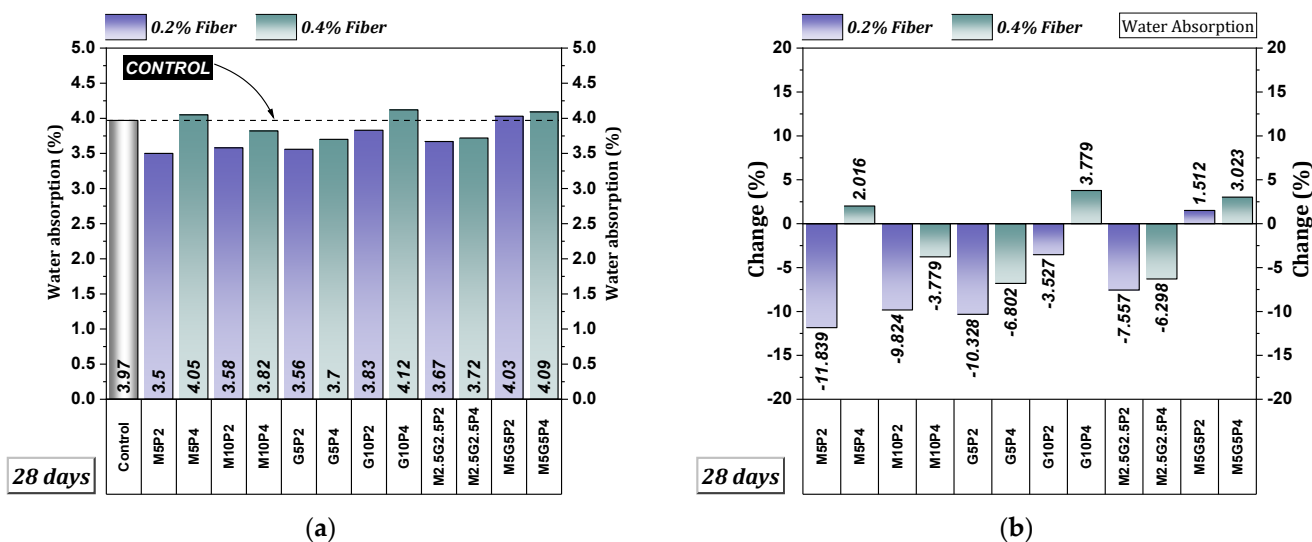


Figure 11. (a) Final water absorption results, (b) Final water absorption changes.

An analysis of the water absorption results in geopolymer mixtures containing glass powder and polypropylene fibers indicates that the combination and dosage of these two components significantly affect water absorption. In the G5P2 mixture, which consists of 5% glass powder and 0.2% polypropylene fibers, water absorption was reduced by 10.328%, likely due to improved adhesion properties and the formation of a denser microstructural framework. Additionally, in the G5P4 mixture with 5% glass powder and an increase in fiber content to 0.4%, a decrease in water absorption of 6.802% was observed, suggesting

enhanced strength and reduced void spaces in the mortar. In the G10P2 mixture containing 10% glass powder and 0.2% polypropylene fibers, the water absorption reduced to 3.527%, which may be attributable to notable changes in the prevailing microstructure. However, in the G10P4 mixture, where a greater fiber content (0.4%) was added while maintaining the same amount of glass powder (10%), a 3.779% increase in water absorption was observed. This increase may result from the additional fibrous structure, which could create more voids and, consequently, elevate the water absorption levels [58]. Therefore, it appears that an optimal ratio of glass powder and polypropylene fibers is necessary to achieve the lowest possible water absorption.

The water absorption results in geopolymer mixtures that contain glass powder, metakaolin, and polypropylene fibers demonstrating the influence of the composition and proportion of these materials on this property. The M2.5G2.5P2 mixture, comprising 2.5% glass powder, 2.5% metakaolin, and 0.2% polypropylene fibers, experienced a reduction in water absorption of 7.557%, which may be attributed to an improved microscopic structure and enhanced cohesion between components. In the M2.5G2.5P4 mixture, with an increase in fiber content to 0.4%, water absorption decreased by 6.298%, indicating further reinforcement of the mortar structure. However, in mixtures M5G5P2 and M5G5P4, with increased quantities of glass powder and metakaolin to 5%, and polypropylene fibers at 0.2% and 0.4%, respectively, water absorption increased by 1.512% and 3.023%. This increase in water absorption may be due to excessive compaction and reduced permeability resulting from the abundance of materials, which creates more void space and leads to an increase in the amount of water absorbed.

5.5. Rapid Chloride Migration Test (RCMT)—28 Days

The results obtained from the RCMT for geopolymer mixtures are reported in Figure 12a. The changes in RCMT values for different mixtures relative to the control mixture are observable in Figure 12b. The RCMT value for the control mixture was recorded as $5.1 \times 10^{-12} \text{ m}^2/\text{s}$. RCMT results for geopolymer mixtures containing metakaolin and polypropylene fibers indicate a variable influence of the material composition on mortar permeability. In mixture M5P2, with 5% metakaolin and 0.2% polypropylene fibers, a 9.804% decrease in RCMT was observed, suggesting this combination can improve the microscopic structure and reduce chloride ion penetration. This reduction may be attributed to increased bonding and decreased void phases within the mortar matrix. The positive effects of using polypropylene fibers on durability of geopolymer concrete were reported by other researchers [58]. Conversely, mixture M5P4, containing 5% metakaolin and 0.4% fibers, exhibited a 5.883% increase in RCMT, indicating that the addition of excess fibers may lead to the formation of weak zones within the mortar, as well as non-uniform material distribution, consequently increasing permeability. A similar trend was observed in mixtures M10P2 and M10P4; while M10P2, with 10% metakaolin and 0.2% fibers, showed a 3.922% decrease in RCMT, M10P4, with 10% metakaolin and 0.4% fibers, experienced a similar increase. Overall, these findings demonstrate that an optimal ratio of metakaolin and polypropylene fibers is essential to enhance the mortar's permeability properties, and higher concentrations can have detrimental effects.

The RCMT results for geopolymer mixtures incorporating glass powder and polypropylene fibers demonstrate a variable influence of material composition on concrete permeability. Mixtures G5P2 and G5P4, containing 5% glass powder, exhibited reductions in RCMT of 7.844% and 3.922%, respectively, indicating enhanced structural integrity and reduced chloride ion ingress. Notably, increasing the polypropylene fiber content from 0.2% to 0.4% in these mixtures did not adversely affect performance. Conversely, the G10P2 mixture (10% glass powder, 0.2% fibers) showed a modest 1.961% decrease in RCMT, suggesting a

negative impact of higher glass powder content on permeability. Furthermore, the G10P4 mixture (10% glass powder, 0.4% fibers) exhibited a significant 11.765% increase in RCMT, indicative of compromised structural integrity due to the high concentrations of both additives. This deterioration is likely attributed to the formation of voids and microcracks resulting from non-uniform distribution of fibers and glass powder, facilitating increased permeability. These findings underscore the critical role of achieving an optimal balance between glass powder and polypropylene fiber content to optimize the mechanical and chemical properties of geopolymer mortar.

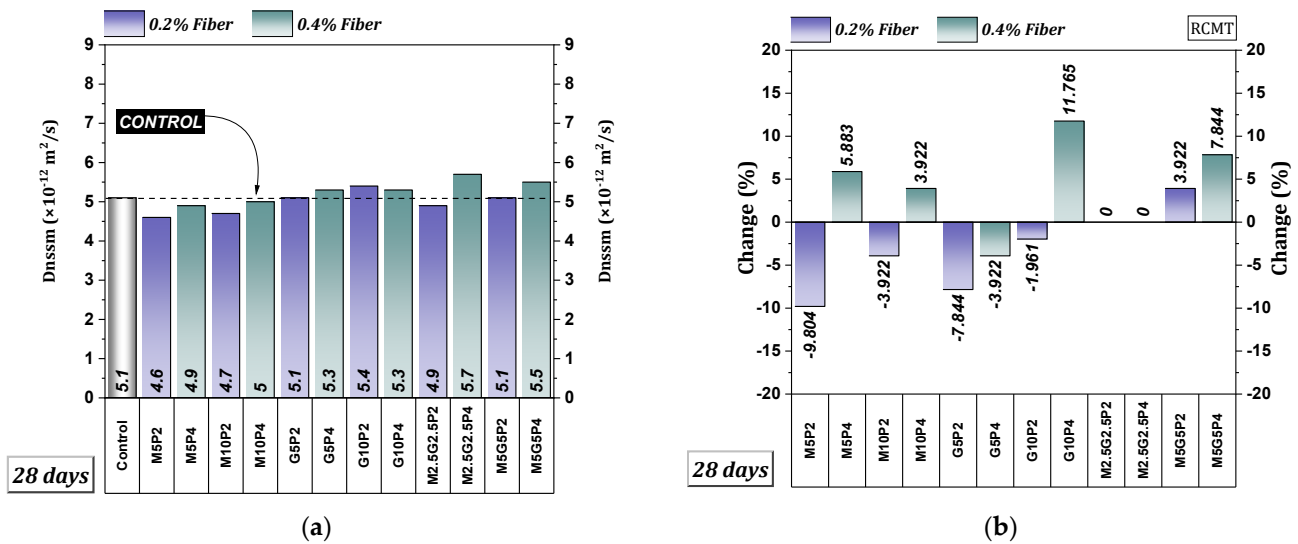


Figure 12. (a) RCMT results. (b) Variation in RCMT results.

An investigation into RCMT findings for geopolymer mortar containing glass powder, metakaolin, and polypropylene fibers reveals the significant influence of material composition on mortar permeability. In mixtures M2.5G2.5P2 and M2.5G2.5P4, despite incorporating equal proportions of glass powder and metakaolin alongside polypropylene fibers, no discernible change in RCMT was observed, indicating a favorable balance within this composition. This phenomenon can be attributed to the formation of a suitable microscopic structure and reduced permeability resulting from the stabilization of constituents. However, in mixtures M5G5P2 and M5G5P4, where the proportions of glass powder and metakaolin were increased, substantial increases of 3.922% and 7.844% in RCMT were detected, respectively. These elevations can be ascribed to the congestion of the mortar matrix and the creation of weak zones arising from high concentrations of admixtures, consequently leading to enhanced permeability and compromised structural integrity. Therefore, it appears that elevated ratios of glass powder and metakaolin may exert a detrimental impact on the permeability characteristics of mortar in this instance, underscoring the necessity of maintaining a balanced admixture composition to optimize the performance of geopolymer mortar.

5.6. Regression Analysis

Figure 13 displays the regression results among various tests of geopolymer mixtures. The regression outcomes indicate that there are significant relationships among the different tests of geopolymer mortar. As shown in Figure 13a, the relationship between compressive strength and flexural strength is represented by the equation $y = 25.861e^{0.0866x}$ with a coefficient of determination $R^2 = 0.8637$, indicating a strong correlation between these two parameters. This suggests that, as compressive strength increases, flexural strength also significantly increases. Additionally, as illustrated in Figure 13b, the relationship

between electrical resistance and final water absorption is represented by the equation $y = 9.0869e^{-0.087x}$ with $R^2 = 0.8472$. This indicates that, with an increase in electrical resistance, water absorption decreases, which may be attributed to a reduction in porosity and an increase in the density of the mortar matrix. Finally, the relationship between RCMT and electrical resistance, represented by a linear equation $y = -0.4436x + 9.528$ with $R^2 = 0.7045$, indicates (as shown in Figure 13c) that as electrical resistance increases, the chloride migration amount decreases. This may be attributed to the enhanced resistance of mortar against the penetration of chloride ions. These regression relationships can serve as valuable tools for predicting and improving the mechanical properties and durability of geopolymer mortar.

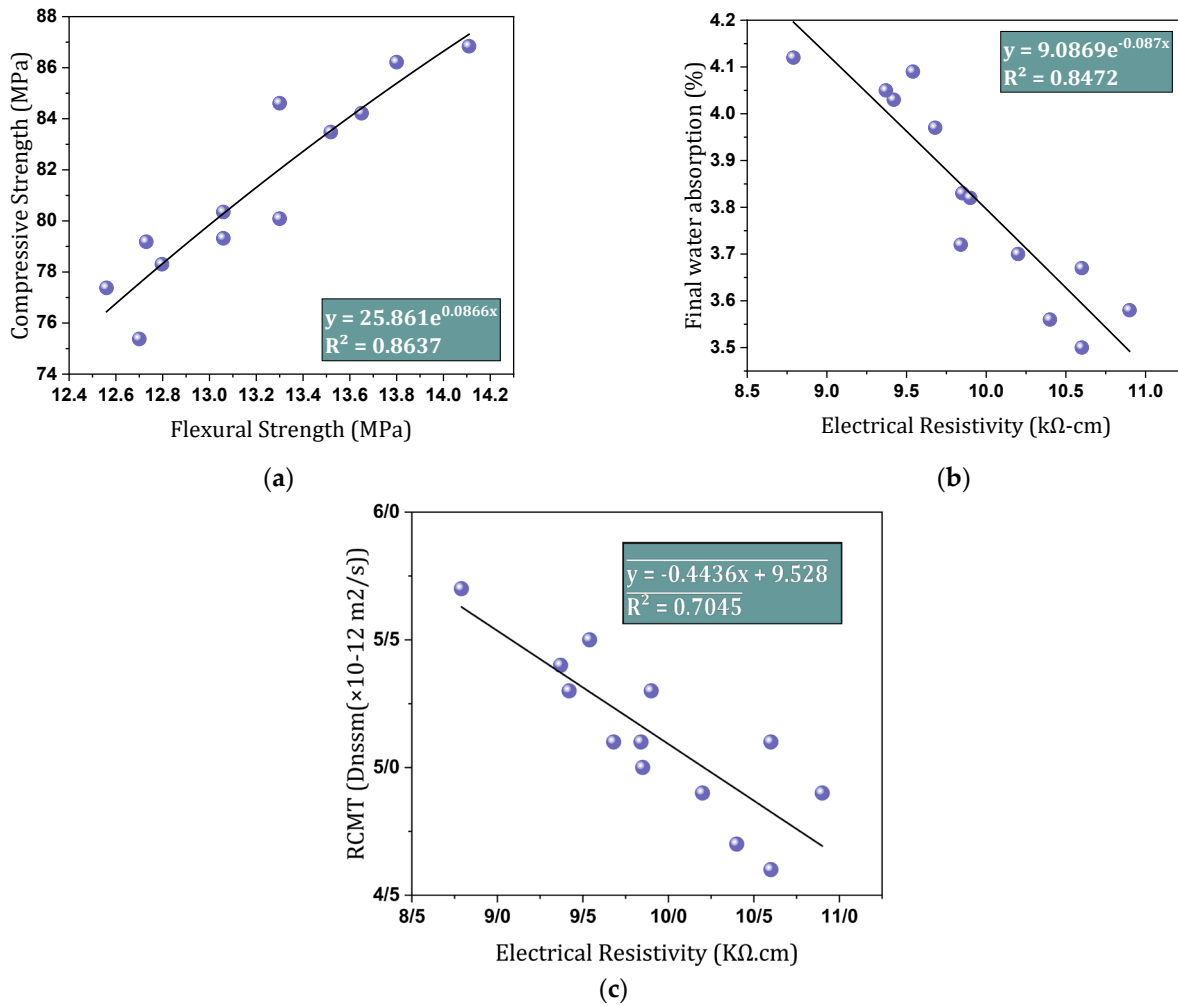


Figure 13. Regression results for different tests. (a) Compressive and flexural strength. (b) Electrical resistivity and final water absorption. (c) Electrical resistivity and RCMT.

5.7. Predicting Compressive Strength Using Fuzzy Logic

Table 6 provides a comprehensive report on the predicted compressive strength results (7 and 28 days) obtained through the FL model, along with the associated prediction errors. Additionally, Figure 14 displays the compressive strength results obtained from laboratory operations and predictions made by the FL model. The prediction error for the compressive strength at 7 and 28 days as determined by the FL model is presented in Figure 15. The results obtained from predicting the compressive strength of geopolymer mortar using the FL model indicate the high accuracy of this model in estimating the mechanical properties of this type of mortar. The prediction errors for compressive strength at 7 days and 28 days

were found to be 0.79% and 0.52%, respectively, demonstrating the model’s capability and accuracy in assessing mortar performance under various conditions. Furthermore, according to Figure 16, the R^2 values for 7-day and 28-day compressive strength were found to be 0.9842 and 0.9884, respectively, indicating a very strong correlation between the experimental results and the FL model predictions. In other words, values close to 1 for R^2 confirm that nearly all the variance in the experimental data is accounted for by the model, highlighting its high capability in simulating mortar behavior. These characteristics enhance the validity and reliability of the FL model in predicting the mechanical behavior of geopolymers mortars, making it a useful tool for the design and optimization of various compositions of these concrete and mortar types. Moreover, the findings may pave the way for future research in related fields concerning sustainable building materials and the optimization of their mechanical properties, particularly in the context of the growing use of bio-based and high-performance materials.

Table 6. Percentage absolute relative errors of predicted and measured compressive strengths by FL model.

Mix Code	Measured Results		FL Results		% Relative Error of FL Model	
	7 Days	28 Days	7 Days	28 Days	7 Days	28 Days
Control	63.412	82.272	63.60	82.40	0.30	0.16
M5P2	62.792	79.316	63.00	79.80	0.33	0.61
M10P2	59.788	77.376	59.50	77.70	0.48	0.42
G5P2	66.752	83.48	66.00	83.50	1.14	0.02
G10P2	66.68	86.84	66.10	85.70	0.88	1.33
M2.5G2.5P2	68.392	80.348	68.50	80.10	0.16	0.31
M5G5P2	65.276	86.216	65.00	85.80	0.42	0.48
M5P4	63.16	79.184	63.00	78.80	0.25	0.49
M10P4	56.948	75.376	57.00	76.20	0.09	1.08
G5P4	66.46	80.088	66.10	79.80	0.54	0.36
G10P4	72.396	84.216	71.30	83.50	1.54	0.86
M2.5G2.5P4	55.632	84.608	57.20	84.60	2.74	0.01
M5G5P4	64.08	78.304	65.00	78.80	1.42	0.63
Average error					0.79	0.52

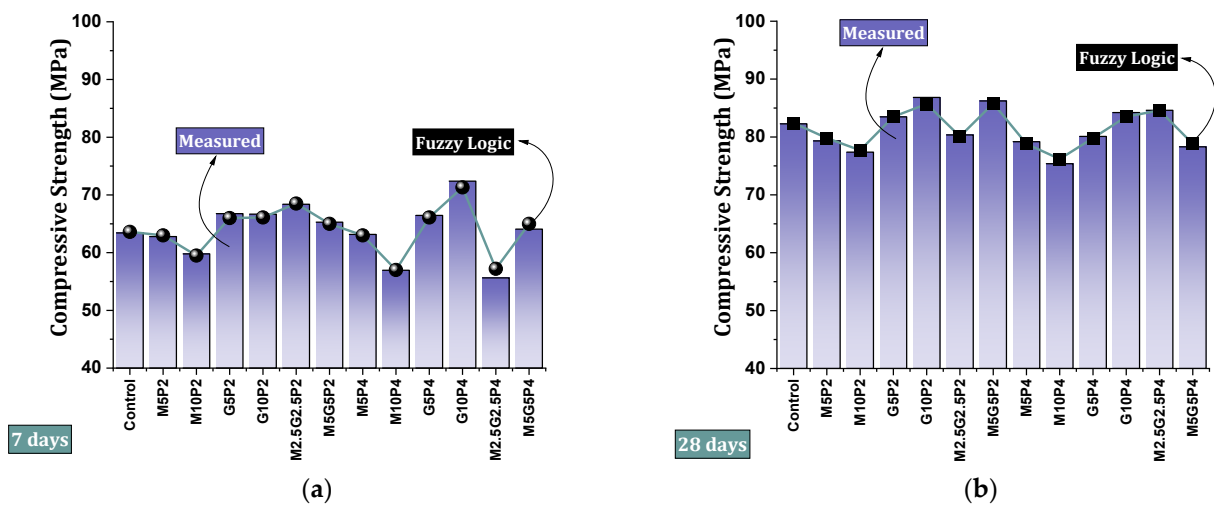


Figure 14. Experimental results and compressive strength predictions using the FL model: (a) 7 days, (b) 28 days.

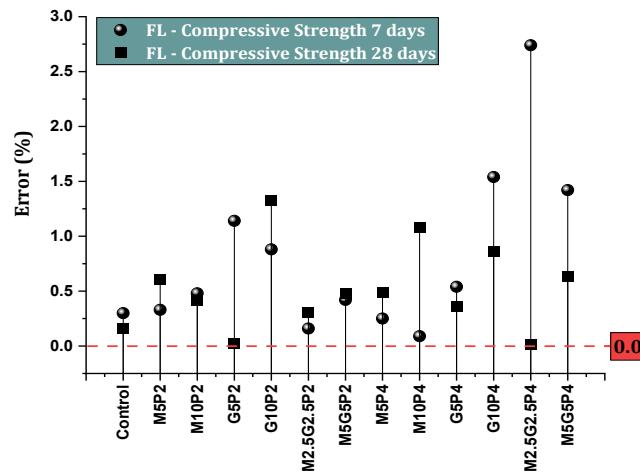


Figure 15. Measurement error using the FL model.

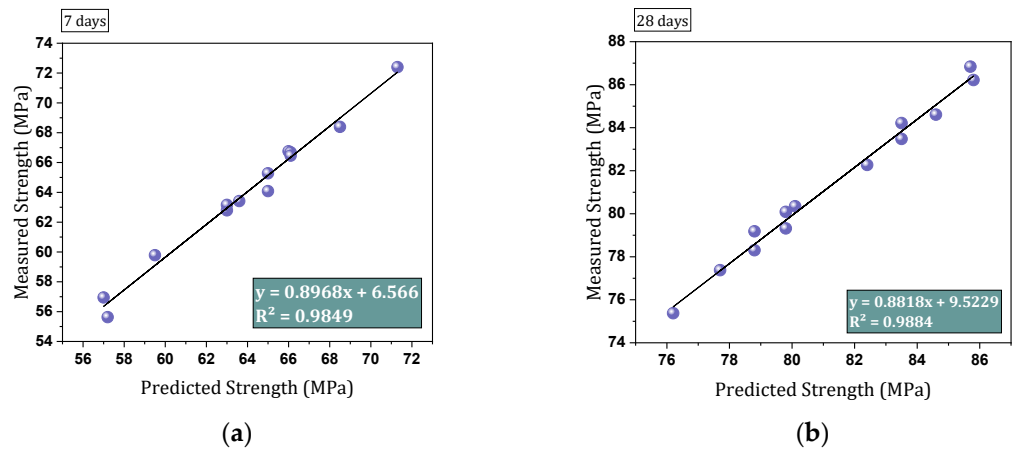


Figure 16. The correlation of the measured and predicted compressive strengths: (a) 7 days, (b) 28 days.

6. Validation of Results

Table 7 presents a summary of the results of research on various geopolymer mortars. The results obtained from the geopolymer mortar developed in this study were found to fall within an acceptable range when compared to previous research, demonstrating alignment with past findings. Particularly, the properties of compressive strength, tensile strength, and flexural strength of the samples were clearly found to be consistent with the results of earlier studies, as presented in the accompanying table. This overlap not only enhances the credibility of the findings but also indicates the reliability of geopolymer mortar incorporating pozzolans and fibers. Moreover, these results confirm the effectiveness and high potential of this type of mortar and concrete in various construction and civil engineering applications. Thus, the outcomes of this research are aligned with recent advancements in the field, effectively showcasing the positive impacts of additive materials on the improvement of geopolymer mortar/concrete properties.

Table 7. Summary of research findings on various geopolymer mixtures.

N.O.	Precursor	Alcaline Activator	Curing Temperature	W (mm)	ST (Min)	CS (MPa)	TS (MPa)	FS (MPa)	Ref.
1	Fly Ash	NaOH + KOH + Na ₂ SiO ₃	-	-	-	24.96–30.11	3.72–4.95	5.22–6.03	[94]
2	Fly Ash	NaOH + Na ₂ SiO ₃	-	240	IST = 405 FST = 570	47.21	-	-	[95]
3	Fly Ash	NaOH + Na ₂ SiO ₃	Ambient temperature	-	IST = 66–112 FST = 160–245	40	-	-	[96]
4	Fly Ash	NaOH + Na ₂ SiO ₃	60–90 °C	710	-	47.54–53.99	-	-	[97]
5	Fly Ash	NaOH + Na ₂ SiO ₃	80 °C	-	-	48	-	-	[98]
6	Fly Ash	NaOH + Na ₂ SiO ₃	75 °C	110–135	-	10–65	-	-	[99]
7	Fly Ash	NaOH + Na ₂ SiO ₃	Ambient temperature	-	-	11.8–29.2	-	-	[100]
8	Fly Ash + Slag + Palm oil fuel ash	NaOH + Na ₂ SiO ₃	65 °C	145–160	-	66	-	7.7	[101]
9	Fly Ash + Slag + Portland cement + Calcium hydroxide	NaOH + Na ₂ SiO ₃	Ambient temperature	-	IST = 110–607 FST = 110–607	26–58	-	-	[102]
10	Fly Ash + Slag	NaOH + Na ₂ SiO ₃	Ambient temperature	-	-	30.5–80.5	8.35	17.95	[103]
11	Fly Ash + Slag + Nano silica	NaOH + Na ₂ SiO ₃	Ambient temperature	-	-	40.28–56.7	-	-	[104]
12	Fly Ash + Slag + High calcium wood ash	NaOH + Na ₂ SiO ₃	-	-	IST = 20–280 FST = 90–360	36.56	-	-	[105]
13	Fly Ash + GGBS + Red Mud	NaOH + Na ₂ SiO ₃	Ambient temperature	-	-	25–39.7	-	3.96–5.45	[106]
14	Fly ash + GGBS + Silica fume	NaOH + Na ₂ SiO ₃	Ambient temperature	-	IST = 18–168 FST = 284–620	9–79	3.3–5.4	4.6–7.4	[107]
15	GGBS	NaOH + Na ₂ SiO ₃	Ambient temperature	654–752	-	31–69	1.66–3.97	-	[108]
16	Algerian Beni Saf natural Pozzolan (BSP)	NaOH + Na ₂ SiO ₃	20, 40, 60, 80 °C	-	-	22.8–38.8	-	5.3–12.4	[109]

Table 7. Cont.

N.O.	Precursor	Alcaline Activator	Curing Temperature	W (mm)	ST (Min)	CS (MPa)	TS (MPa)	FS (MPa)	Ref.	
17	Steel, Polypropylene	Fly Ash + GGBS	NaOH + Na ₂ SiO ₃	22 ± 2 °C	-	-	59–65	5.23–3.78	-	[50]
18	Steel, PVA	Fly Ash + GGBS	NaOH + Na ₂ SiO ₃	20 °C	-	-	42.2–54.3	-	5.3–7.8	[110]
19	Basalt	Fly Ash + GGBS+ Silica Fume	NaOH + Na ₂ SiO ₃	25 ± 5 °C	69–164	-	46.60–57.97	3.91–4.81	-	[111]
20	Steel	Fly Ash + GGBS	NaOH + Na ₂ SiO ₃	20 ± 3 °C	51–198	-	37.4–56.4	2.99–4.79	-	[112]

ST = Setting Time, CS = Compressive Strength, TS = Tensile Strength, FS = Flexural Strength, IST = Initial Setting Time, FST = Final Setting Time, W = Workability.

7. Conclusions

In this study, the mechanical properties and durability of fiber-reinforced geopolymer mortars containing metakaolin and glass powder in chloride environments were investigated. Based on the findings from the conducted experiments, the following conclusions can be drawn:

- The incorporation of glass powder at 5% and 10% levels positively influences the 7-day compressive strength of geopolymer concrete, with strength increases ranging from 4.8% to 14.2%. Conversely, metakaolin substitution at 5% and 10% levels leads to a decline in compressive strength. In hybrid mixtures, the combination of metakaolin, glass powder, and polypropylene fibers shows varied effects, with some compositions demonstrating strength improvements while others experience performance degradation. At 28 days, the incorporation of metakaolin consistently reduced the compressive strength of geopolymer concrete, with strength decreases becoming more pronounced as metakaolin content increased. Glass powder showed varying effects, with 5% and 10% additions yielding modest strength improvements. The impact of polypropylene fibers was complex, with fiber content of 0.2% generally improving strength, while 0.4% fiber content often led to strength reductions. The performance of hybrid mixtures was notably sensitive to the precise proportions of metakaolin, glass powder, and polypropylene fibers.
- The incorporation of metakaolin, glass powder, and polypropylene fibers significantly influences the 28-day flexural strength of geopolymer concrete. Optimal performance was achieved with specific combinations, notably mixtures containing 5% metakaolin with 0.2% fibers and 10% glass powder with 0.2% fibers, which demonstrated substantial increases in flexural strength. The research highlights the critical importance of maintaining precise proportions of these additives, as excessive fiber content can potentially disrupt the mortar matrix and compromise mechanical properties.
- Electrical resistivity in geopolymer mortar is significantly influenced by the ratios of metakaolin, glass powder, and polypropylene fibers. Optimal mixtures, such as M5P2 and M2.5G2.5P2, achieve 9.505% increases in resistivity due to improved particle interaction. Conversely, excessive amounts of glass powder in G10P4 lead to a 9.194% decrease. Therefore, maintaining precise material ratios is crucial for enhancing electrical performance and structural integrity.
- The use of glass powder and metakaolin in the geopolymer mortar mixture as a partial replacement for slag results in decreased permeability and consequently reduced ultimate water absorption. Optimal mixtures, such as M5P2 and G5P2, demonstrate significant reductions in water absorption due to improved microstructural properties and enhanced matrix adhesion. However, excessive fiber content or high proportions of metakaolin and glass powder can lead to increased water absorption, indicating the necessity of achieving precise material ratios to minimize water ingress and improve overall performance. The effect of glass powder on reducing water absorption is more significant compared to that of metakaolin.
- The proportions of metakaolin, glass powder, and polypropylene fibers play a crucial role in the chloride ion permeability of geopolymer concrete. Mixtures with balanced amounts, such as those containing 5% metakaolin and 0.2% polypropylene fibers, achieved significant reductions in permeability due to an enhanced microstructure. However, using too much fiber or high levels of these additives can actually increase permeability. This highlights the necessity for careful mix design to optimize performance and durability against chloride ion penetration.
- The material composition significantly impacts the chloride ion permeability of geopolymer concrete. Mixtures with 5% metakaolin and 0.2% polypropylene fibers

showed a 9.804% reduction in permeability, enhancing microstructural integrity. However, when using 0.4% fibers, permeability increased by 5.883%. Similarly, mixtures with 5% glass powder also reduced permeability, while increasing the additive content led to adverse effects. Maintaining balanced proportions is crucial for optimizing permeability performance and ensuring the durability of geopolymer mortar.

- The results indicate that the FL model serves as a robust and accurate tool for predicting the compressive strength of geopolymers. The high accuracy of this model is evidenced by low prediction errors (approximately 0.79% and 0.52% for 7-day and 28-day compressive strengths, respectively) and an R^2 value close to 1 in the regression between experimental and predicted results, demonstrating its capability to elucidate and simulate the mechanical behavior of this type of mortar. Furthermore, the findings of this research could aid in optimizing the compositions of geopolymer mortars and enhancing the sustainability of building materials, which is crucial for improving the performance and stability of modern construction networks, particularly in the efficient use of bio-based materials.

8. Future Research Recommendations

This study opens several promising avenues for further investigation in geopolymer mortar development:

1. It would be beneficial to assess how these geopolymer mortars perform under short-term dynamic loads, such as those experienced in seismic events or heavy traffic conditions. Understanding the material's response to such stresses will provide deeper insights into its applicability in critical infrastructure.
2. Investigating the effects of functionalized nanomaterials, such as graphene oxide, could lead to further enhancements in mechanical properties and durability. The inclusion of nanotechnology in construction materials is a burgeoning field that warrants exploration to optimize performance.
3. Future studies could also focus on the lifecycle assessment of geopolymer concrete, evaluating its overall carbon footprint compared to traditional concrete mixtures. Understanding the environmental benefits or drawbacks will be crucial for promoting the adoption of geopolymer technologies.
4. Long-term durability studies: Extended research into the long-term durability of these geopolymer mortars in various environmental conditions will provide essential data for practical applications. This includes exposure to humidity, temperature fluctuations, and aggressive chemical environments.
5. Future research should explore advanced predictive modeling techniques for geopolymer concrete, focusing on quantum machine learning, physics-informed neural networks, and multi-scale generative models that integrate domain-specific material science principles to enable more sophisticated prediction methodologies beyond traditional statistical learning.

Author Contributions: Conceptualization, M.A.M.L. and A.S.; methodology, M.A.M.L. and M.M.M.; software, M.A.M.L. and A.S.; validation, M.A.M.L., M.M.M. and A.S.; formal analysis, M.M.M. and A.S.; investigation, M.A.M.L., M.M.M. and A.S.; resources, M.A.M.L., M.M.M. and A.S.; data curation, M.A.M.L. and A.S.; writing—original draft preparation, M.A.M.L., M.M.M. and A.S.; writing—review and editing, M.A.M.L., M.M.M. and A.S.; visualization, M.M.M. and A.S.; supervision, M.A.M.L. and M.K.; project administration, M.A.M.L. All authors have read and agreed to the published version of the manuscript.

Funding: This research received no external funding.

Data Availability Statement: The data set analyzed during the current study is available and can be provided upon request.

Conflicts of Interest: The authors declare no conflicts of interest.

References

1. Mohtasham Moein, M.; Rahmati, K.; Mohtasham Moein, A.; Rigby, S.E.; Saradar, A.; Karakouzian, M. Utilizing Construction and Demolition Waste in Concrete as a Sustainable Cement Substitute: A Comprehensive Study on Behavior Under Short-Term Dynamic and Static Loads via Laboratory and Numerical Analysis. *J. Build. Eng.* **2024**, *97*, 110778. [[CrossRef](#)]
2. Mohtasham Moein, M.; Rahmati, K.; Saradar, A.; Moon, J.; Karakouzian, M. A Critical Review Examining the Characteristics of Modified Concretes with Different Nanomaterials. *Materials* **2024**, *17*, 409. [[CrossRef](#)]
3. Beshkari, M.; Amani, B.; Rahmati, K.; Mohtasham Moein, M.; Saradar, A.; Karakouzian, M. Synergistic Effects of Pozzolan and Carbon Fibers on the Performance of Self-Consolidating Concrete under Plastic Shrinkage and Dynamic Loading. *Innov. Infrastruct. Solut.* **2024**, *9*, 160. [[CrossRef](#)]
4. Sedić, K.; Ukrainczyk, N.; Mandić, V.; Gaurina-Međimurec, N. Carbonation Study of New Calcium Aluminate Cement-Based CO₂ Injection Well Sealants. *Constr. Build. Mater.* **2024**, *419*, 135517. [[CrossRef](#)]
5. Kaptan, K.; Cunha, S.; Aguiar, J. A Review: Construction and Demolition Waste as a Novel Source for CO₂ Reduction in Portland Cement Production for Concrete. *Sustainability* **2024**, *16*, 585. [[CrossRef](#)]
6. Assi, L.N.; Eddie Deaver, E.; Ziehl, P. Effect of Source and Particle Size Distribution on the Mechanical and Microstructural Properties of Fly Ash-Based Geopolymer Concrete. *Constr. Build. Mater.* **2018**, *167*, 372–380. [[CrossRef](#)]
7. Mohammad Nezhad Ayandeh, M.H.; Ghodousian, O.; Mohammad Nezhad, H.; Mohtasham Moein, M.; Saradar, A.; Karakouzian, M. Steel Slag and Zeolite as Sustainable Pozzolans for UHPC: An Experimental Study of Binary and Ternary Pozzolan Mixtures under Various Curing Conditions. *Innov. Infrastruct. Solut.* **2024**, *9*, 265. [[CrossRef](#)]
8. Mansoori, A.; Mohtasham Moein, M.; Mohseni, E. Effect of Micro Silica on Fiber-Reinforced Self-Compacting Composites Containing Ceramic Waste. *J. Compos. Mater.* **2020**, *55*, 95–107. [[CrossRef](#)]
9. Sun, J.; Zunino, F.; Scrivener, K. Hydration and Phase Assemblage of Limestone Calcined Clay Cements (LC3) with Clinker Content below 50%. *Cem. Concr. Res.* **2024**, *177*, 107417. [[CrossRef](#)]
10. Saradar, A.; Reza khani, Y.; Rahmati, K.; Johari Majd, F.; Mohtasham Moein, M.; Karakouzian, M. Investigating the Properties and Microstructure of High-Performance Cement Composites with Nano-Silica, Silica Fume, and Ultra-Fine TiO₂. *Innov. Infrastruct. Solut.* **2024**, *9*, 84. [[CrossRef](#)]
11. Octaviani, Y.N.; Budihardjo, M.A.; Sumiyati, S. The Impact of Food Waste Mitigation with Black Soldier Fly Assistance on Climate Change in Indonesia—A Systematic Review. *Ecol. Eng. Environ. Technol.* **2024**, *25*, 60–72. [[CrossRef](#)]
12. Zhou, S.; Huang, P.; Wang, L.; Hu, K.; Huang, G.; Hu, P. Robust Changes in Global Subtropical Circulation under Greenhouse Warming. *Nat. Commun.* **2024**, *15*, 96. [[CrossRef](#)] [[PubMed](#)]
13. Phummiphan, I.; Horpibulsuk, S.; Rachan, R.; Arulrajah, A.; Shen, S.L.; Chindaprasirt, P. High Calcium Fly Ash Geopolymer Stabilized Lateritic Soil and Granulated Blast Furnace Slag Blends as a Pavement Base Material. *J. Hazard. Mater.* **2018**, *341*, 257–267. [[CrossRef](#)] [[PubMed](#)]
14. Moein, M.M.; Saradar, A.; Rahmati, K.; Reza khani, Y.; Ashkan, S.A.; Karakouzian, M. Reliability Analysis and Experimental Investigation of Impact Resistance of Concrete Reinforced with Polyolefin Fiber in Different Shapes, Lengths, and Doses. *J. Build. Eng.* **2023**, *69*, 106262. [[CrossRef](#)]
15. Tahmouresi, B.; Nemati, P.; Asadi, M.A.; Saradar, A.; Mohtasham Moein, M. Mechanical Strength and Microstructure of Engineered Cementitious Composites: A New Configuration for Direct Tensile Strength, Experimental and Numerical Analysis. *Constr. Build. Mater.* **2021**, *269*, 121361. [[CrossRef](#)]
16. Heyran Najafi, M.R.; Saradar, A.; Mohtasham Moein, M.; Karakouzian, M. Investigation Mechanical Characteristics and Permeability of Concrete with Pozzolanic Materials: A Sustainable Approach. *Multiscale Multidiscip. Model. Exp. Des.* **2024**, *7*, 5051–5078. [[CrossRef](#)]
17. Tajasosi, S.; Saradar, A.; Barandoust, J.; Mohtasham Moein, M.; Zeinali, R.; Karakouzian, M. Multi-Criteria Risk Analysis of Ultra-High Performance Concrete Application in Structures. *CivilEng* **2023**, *4*, 1016–1035. [[CrossRef](#)]
18. Witte, A.; Garg, N. Quantifying the Global Warming Potential of Low Carbon Concrete Mixes: Comparison of Existing Life Cycle Analysis Tools. *Case Stud. Constr. Mater.* **2024**, *20*, e02832. [[CrossRef](#)]
19. Chen, C.; Habert, G.; Bouzidi, Y.; Jullien, A. Environmental Impact of Cement Production: Detail of the Different Processes and Cement Plant Variability Evaluation. *J. Clean. Prod.* **2010**, *18*, 478–485. [[CrossRef](#)]
20. Nabighods, K.; Saradar, A.; Mohtasham Moein, M.; Mirgozar Langaroudi, M.A.; Byzyka, J.; Karakouzian, M. Evaluation of Self-Compacting Concrete Containing Pozzolan (Zeolite, Metakaolin & Silica Fume) and Polypropylene Fiber against Sulfate Attacks with Different PH: An Experimental Study. *Innov. Infrastruct. Solut.* **2023**, *9*, 1. [[CrossRef](#)]

21. Sadrmomtazi, A.; Tahmouresi, B.; Saradar, A. Effects of Silica Fume on Mechanical Strength and Microstructure of Basalt Fiber Reinforced Cementitious Composites (BFRCC). *Constr. Build. Mater.* **2018**, *162*, 321–333. [[CrossRef](#)]
22. Koushkbaghi, M.; Alipour, P.; Tahmouresi, B.; Mohseni, E.; Saradar, A.; Sarker, P.K. Influence of Different Monomer Ratios and Recycled Concrete Aggregate on Mechanical Properties and Durability of Geopolymer Concretes. *Constr. Build. Mater.* **2019**, *205*, 519–528. [[CrossRef](#)]
23. Sadrmomtazi, A.; Khameneh, N.G.; Khoshkbijari, R.K.; Amooie, M. A Study on the Durability of the Slag-Based Geopolymer Concretes Containing Binary Solid Mixtures in Corrosive Environments. *Rev. Romana Mater./Rom. J. Mater.* **2021**, *51*, 195–206.
24. Mousavinejad, S.H.G.; Saradar, A.; Jabbari, M.; Moein, M.M. Evaluation of Fresh and Hardened Properties of Self-Compacting Concrete Containing Different Percentages of Waste Tiles. *J. Build. Pathol. Rehabil.* **2023**, *8*, 81. [[CrossRef](#)]
25. Azunna, S.U.; Aziz, F.N.A.B.A.; Abbas Al-Ghazali, N.; Rashid, R.S.M.; Bakar, N.A. Review on the Mechanical Properties of Rubberized Geopolymer Concrete. *Clean. Mater.* **2024**, *11*, 100225. [[CrossRef](#)]
26. Zaid, O.; Abdulwahid Hamah Sor, N.; Martínez-García, R.; de Prado-Gil, J.; Mohamed Elhadi, K.; Yosri, A.M. Sustainability Evaluation, Engineering Properties and Challenges Relevant to Geopolymer Concrete Modified with Different Nanomaterials: A Systematic Review. *Ain Shams Eng. J.* **2024**, *15*, 102373. [[CrossRef](#)]
27. Ekinci, E.; Türkmen, İ.; Kantarci, F.; Karakoç, M.B. The Improvement of Mechanical, Physical and Durability Characteristics of Volcanic Tuff Based Geopolymer Concrete by Using Nano Silica, Micro Silica and Styrene-Butadiene Latex Additives at Different Ratios. *Constr. Build. Mater.* **2019**, *201*, 257–267. [[CrossRef](#)]
28. Ramesh, G. Geopolymer Concrete: A Review. *Indian J. Struct. Eng.* **2021**, *1*, 5–8. [[CrossRef](#)]
29. Şahmaran, M.; Yıldırım, G.; Shaikh, F. *Recent Advances in Nano-Tailored Multi-Functional Cementitious Composites*; Elsevier: Amsterdam, The Netherlands, 2022.
30. Sarker, P.K.; Kelly, S.; Yao, Z. Effect of Fire Exposure on Cracking, Spalling and Residual Strength of Fly Ash Geopolymer Concrete. *Mater. Des.* **2014**, *63*, 584–592. [[CrossRef](#)]
31. Karakoç, M.B.; Türkmen, İ.; Maraş, M.M.; Kantarci, F.; Demirboğa, R.; Uçur Toprak, M. Mechanical Properties and Setting Time of Ferrochrome Slag Based Geopolymer Paste and Mortar. *Constr. Build. Mater.* **2014**, *72*, 283–292. [[CrossRef](#)]
32. Younis, K.H.; Salihi, K.A.; Ibrahim, T.K. An Overview of Geo-Polymer Concrete Including Recycled Aggregate. *Int. J. Sci. Technol. Res.* **2020**, *9*, 6239–6245.
33. Skariah Thomas, B.; Yang, J.; Bahurudeen, A.; Chinnu, S.N.; Abdalla, J.A.; Hawileh, R.A.; Hamada, H.M. Geopolymer Concrete Incorporating Recycled Aggregates: A Comprehensive Review. *Clean. Mater.* **2022**, *3*, 100056. [[CrossRef](#)]
34. Singh, N.B.; Kumar, M.; Rai, S. Geopolymer Cement and Concrete: Properties. *Mater. Today Proc.* **2020**, *29*, 743–748. [[CrossRef](#)]
35. Hassan, A.; Arif, M.; Shariq, M. Use of Geopolymer Concrete for a Cleaner and Sustainable Environment—A Review of Mechanical Properties and Microstructure. *J. Clean. Prod.* **2019**, *223*, 704–728. [[CrossRef](#)]
36. Yu, M.; Wang, T.; Chi, Y.; Li, D.; Li, L.Y.; Shi, F. Residual Mechanical Properties of GGBS-FA-SF Blended Geopolymer Concrete after Exposed to Elevated Temperatures. *Constr. Build. Mater.* **2024**, *411*, 134378. [[CrossRef](#)]
37. Hassan, M.K.; Ibrahim, M.I.; Shill, S.K.; Al-Deen, S. Mechanical Properties of Rubberised Geopolymer Concrete. *Materials* **2024**, *17*, 1031. [[CrossRef](#)]
38. Duxson, P.; Fernández-Jiménez, A.; Provis, J.L.; Lukey, G.C.; Palomo, A.; Van Deventer, J.S.J. Geopolymer Technology: The Current State of the Art. *J. Mater. Sci.* **2007**, *42*, 2917–2933. [[CrossRef](#)]
39. Wang, Y.; Liu, X.; Zhang, W.; Li, Z.; Zhang, Y.; Li, Y.; Ren, Y. Effects of Si/Al Ratio on the Efflorescence and Properties of Fly Ash Based Geopolymer. *J. Clean. Prod.* **2020**, *244*, 118852. [[CrossRef](#)]
40. Kumar, H.; Prasad, R.; Srivastava, A.; Vashista, M.; Khan, M.Z. Utilisation of Industrial Waste (Fly Ash) in Synthesis of Copper Based Surface Composite through Friction Stir Processing Route for Wear Applications. *J. Clean. Prod.* **2018**, *196*, 460–468. [[CrossRef](#)]
41. *Chinese Standard GB/T 29423*; Alkali-Activated Slag-Fly Ash Concrete for Anticorrosive Cement Products. Standardization Administration of China: Beijing, China, 2012.
42. *British Standard PAS 8820: Construction Materials*; Alkali-Activated Cementitious Material and Concrete. Specification. British Standards Institution: London, UK, 2016.
43. *Ukrainian Standard RSN 336-84*; *Republican Building Norms for Production and Use of Slag Alkaline Binders, Concretes and Structures*; State Committee for Construction Affairs of the Ukrainian SSR: Kiev, Ukraine, 1984.
44. Yang, W.; Zhu, P.; Liu, H.; Wang, X.; Ge, W.; Hua, M. Resistance to Sulfuric Acid Corrosion of Geopolymer Concrete Based on Different Binding Materials and Alkali Concentrations. *Materials* **2021**, *14*, 7109. [[CrossRef](#)]
45. Zaib, S.; Asif, S.H.; Rehman, A.; Nawaz, A.; Ahmad, T.; Ejaz, M.M.; Bibi, N.; Younas, M.A. Current Trends in Geopolymer Concrete's Resistance to Chloride Ion Attack. *Eur. J. Appl. Sci. Eng. Technol.* **2024**, *2*, 177–185. [[CrossRef](#)] [[PubMed](#)]
46. Barbhuiya, S.; Pang, E. Strength and Microstructure of Geopolymer Based on Fly Ash and Metakaolin. *Materials* **2022**, *15*, 3732. [[CrossRef](#)] [[PubMed](#)]

47. Noushini, A.; Hastings, M.; Castel, A.; Aslani, F. Mechanical and Flexural Performance of Synthetic Fibre Reinforced Geopolymer Concrete. *Constr. Build. Mater.* **2018**, *186*, 454–475. [[CrossRef](#)]
48. Widiana, N.; Satyarno, I.; Siswosukarto, S. The Effect of Polypropylene Fiber and Steel Fiber on Geopolymer Concrete. *J. Tek. Sipil Dan Perenc.* **2023**, *25*, 71–80. [[CrossRef](#)]
49. Wang, T.; Fan, X.; Gao, C.; Qu, C.; Liu, J.; Yu, G. The Influence of Fiber on the Mechanical Properties of Geopolymer Concrete: A Review. *Polymers* **2023**, *15*, 827. [[CrossRef](#)]
50. Chen, C.; Zhang, X.; Hao, H. Dynamic Tensile Properties of Geopolymer Concrete and Fibre Reinforced Geopolymer Concrete. *Constr. Build. Mater.* **2023**, *393*, 132159. [[CrossRef](#)]
51. Rahmati, K.; Saradar, A.; Mohtasham Moein, M.; Sardrinejad, I.; Bristow, J.; Yavari, A.; Karakouzian, M. Evaluation of Engineered Cementitious Composites (ECC) Containing Polyvinyl Alcohol (PVA) Fibers under Compressive, Direct Tensile, and Drop-Weight Test. *Multiscale Multidiscip. Model. Exp. Des.* **2022**, *6*, 147–164. [[CrossRef](#)]
52. Mohtasham Moein, M.; Saradar, A.; Rahmati, K.; Hatami Shirkouh, A.; Sadrinejad, I.; Aramali, V.; Karakouzian, M. Investigation of Impact Resistance of High-Strength Portland Cement Concrete Containing Steel Fibers. *Materials* **2022**, *15*, 7157. [[CrossRef](#)]
53. Liu, X.; Wang, S.; Han, F.; Qin, J.; Lu, L.; Xue, Q.; Ji, Y. Mechanical Relationship between Compressive Strength and Sulfate Erosion Depth of Basalt Fiber Reinforced Concrete. *Constr. Build. Mater.* **2024**, *411*, 134412. [[CrossRef](#)]
54. Wang, H.; He, X.; Zhou, M.; Wei, B.; Wu, W.; Zhou, G.; He, J. A Study on the Tensile Fracture Behavior of Polypropylene Fiber Reinforced Concrete Based on a Microscale Model. *Constr. Build. Mater.* **2024**, *417*, 135291. [[CrossRef](#)]
55. Wijesinghe, K.A.P.; Gunasekara, C.; Law, D.W.; Hidallana-Gamage, H.D.; Wanasekara, N.; Wang, L. Thermal and Acoustic Performance in Textile Fibre-Reinforced Concrete: An Analytical Review. *Constr. Build. Mater.* **2024**, *412*, 134879. [[CrossRef](#)]
56. ACI Committee 544 Report on Fiber Reinforced Concrete. *Concr. Int.* **2002**, *6*, 15–27.
57. Sathanandam, T.; Awoyera, P.O.; Vijayan, V.; Sathishkumar, K. Low Carbon Building: Experimental Insight on the Use of Fly Ash and Glass Fibre for Making Geopolymer Concrete. *Sustain. Environ. Res.* **2017**, *27*, 146–153. [[CrossRef](#)]
58. Yavana Rani, S.; Saleh Nusari, M.; bin Non, J.; Poddar, S.; Bhaumik, A. Durability of Geopolymer Concrete with Addition of Polypropylene Fibre. *Mater. Today Proc.* **2022**, *56*, 2846–2851. [[CrossRef](#)]
59. Şahin, F.; Uysal, M.; Canpolat, O.; Aygörmez, Y.; Cosgun, T.; Dehghanpour, H. Effect of Basalt Fiber on Metakaolin-Based Geopolymer Mortars Containing Rilem, Basalt and Recycled Waste Concrete Aggregates. *Constr. Build. Mater.* **2021**, *301*, 124113. [[CrossRef](#)]
60. Si, R.; Dai, Q.; Guo, S.; Wang, J. Mechanical Property, Nanopore Structure and Drying Shrinkage of Metakaolin-Based Geopolymer with Waste Glass Powder. *J. Clean. Prod.* **2020**, *242*, 118502. [[CrossRef](#)]
61. Tho-In, T.; Sata, V.; Boonserm, K.; Chindaprasirt, P. Compressive Strength and Microstructure Analysis of Geopolymer Paste Using Waste Glass Powder and Fly Ash. *J. Clean. Prod.* **2018**, *172*, 2892–2898. [[CrossRef](#)]
62. Vafaei, M.; Allahverdi, A.; Dong, P.; Bassim, N. Acid Attack on Geopolymer Cement Mortar Based on Waste-Glass Powder and Calcium Aluminate Cement at Mild Concentration. *Constr. Build. Mater.* **2018**, *193*, 363–372. [[CrossRef](#)]
63. Mohtasham Moein, M.; Saradar, A.; Rahmati, K.; Ghasemzadeh Mousavinejad, S.H.; Bristow, J.; Aramali, V.; Karakouzian, M. Predictive Models for Concrete Properties Using Machine Learning and Deep Learning Approaches: A Review. *J. Build. Eng.* **2023**, *63*, 105444. [[CrossRef](#)]
64. Saradar, A.; Nemati, P.; Paskiabi, A.S.; Moein, M.M.; Moez, H.; Vishki, E.H. Prediction of Mechanical Properties of Lightweight Basalt Fiber Reinforced Concrete Containing Silica Fume and Fly Ash: Experimental and Numerical Assessment. *J. Build. Eng.* **2020**, *32*, 101732. [[CrossRef](#)]
65. Mohtasham Moein, M.; Soliman, A. Predicting the Compressive Strength of Alkali-Activated Concrete Using Various Data Mining Methods. In *Proceedings of the Canadian Society of Civil Engineering Annual Conference*; Springer Nature: Singapore, 2022; pp. 317–326.
66. Mohtasham Moein, M.; Mousavi, S.Y.; Madandoust, R.; Naser Saeid, H.N.S. The Impact Resistance of Steel Fiber Reinforcement Concrete under Different Curing Conditions: Experimental and Statistical Analysis. *J. Civil. Environ. Eng.* **2019**, *49*, 109–121. [[CrossRef](#)]
67. Sadrmomtazi, A.; Sobhani, J.; Mirgozar, M.A. Modeling Compressive Strength of EPS Lightweight Concrete Using Regression, Neural Network and ANFIS. *Constr. Build. Mater.* **2013**, *42*, 205–216. [[CrossRef](#)]
68. Sobhani, J.; Ejtemaei, M.; Sadrmomtazi, A.; Mirgozar, M.A. MODELING FLEXURAL STRENGTH OF EPS LIGHTWEIGHT CONCRETE USING REGRESSION, NEURAL NETWORK AND ANFIS. *Int. J. Optim. Civ. Eng.* **2019**, *9*, 313–329.
69. Abdellatief, M.; Wong, L.S.; Din, N.M.; Mo, K.H.; Ahmed, A.N.; El-Shafie, A. Evaluating Enhanced Predictive Modeling of Foam Concrete Compressive Strength Using Artificial Intelligence Algorithms. *Mater. Today Commun.* **2024**, *40*, 110022. [[CrossRef](#)]
70. Rathnayaka, M.; Karunasinghe, D.; Gunasekara, C.; Wijesundara, K.; Lokuge, W.; Law, D.W. Machine Learning Approaches to Predict Compressive Strength of Fly Ash-Based Geopolymer Concrete: A Comprehensive Review. *Constr. Build. Mater.* **2024**, *419*, 135519. [[CrossRef](#)]

71. Alaneme, G.U.; Olonade, K.A.; Esenogho, E. Critical Review on the Application of Artificial Intelligence Techniques in the Production of Geopolymer-Concrete. *SN Appl. Sci.* **2023**, *5*, 217.
72. Wang, Y.; Iqtidar, A.; Amin, M.N.; Nazar, S.; Hassan, A.M.; Ali, M. Predictive Modelling of Compressive Strength of Fly Ash and Ground Granulated Blast Furnace Slag Based Geopolymer Concrete Using Machine Learning Techniques. *Case Stud. Constr. Mater.* **2024**, *20*, e03130. [[CrossRef](#)]
73. Van Dao, D.; Trinh, S.H.; Ly, H.B.; Pham, B.T. Prediction of Compressive Strength of Geopolymer Concrete Using Entirely Steel Slag Aggregates: Novel Hybrid Artificial Intelligence Approaches. *Appl. Sci.* **2019**, *9*, 1113. [[CrossRef](#)]
74. Ali, T.; El Ouni, M.H.; Qureshi, M.Z.; Islam, A.B.M.S.; Mahmood, M.S.; Ahmed, H.; Ajwad, A. A Systematic Literature Review of AI-Based Prediction Methods for Self-Compacting, Geopolymer, and Other Eco-Friendly Concrete Types: Advancing Sustainable Concrete. *Constr. Build. Mater.* **2024**, *440*, 137370. [[CrossRef](#)]
75. Siva Krishna, A.; Ranga Rao, V. Strength Prediction of Geopolymer Concrete Using FUZZY. *Int. J. Recent. Technol. Eng.* **2019**, *7*, 661–667.
76. Terrones-Saeta, J.M.; Fortes, J.C.; Luís, A.T.; Aroba, J.; Díaz-Curiel, J.; Romero, E.; Grande, J.A. Fuzzy Logic Tools Application to the Characterization of Stress–Strain Processes in Waste Construction Dam Geopolymers: A New Circular Mining. *Materials* **2022**, *15*, 8793. [[CrossRef](#)] [[PubMed](#)]
77. Crippa, M.; Guizzardi, D.; Pagani, F.; Banja, M.; Muntean, M.; Schaaf, E.; Becker, W.; Monforti-Ferrario, F.; Quadrelli, R.; Riskey Martin, A.; et al. GHG emissions of all world countries. *Publ. Off. Eur. Union.* **2021**. [[CrossRef](#)]
78. ASTM C33/C33M-16; Standard Specification for Concrete Aggregates. ASTM International: West Conshohocken, PA, USA, 2016.
79. C109/C109M-05; Standard Test Method for Compressive Strength of Hydraulic Cement Mortars. ASTM International: West Conshohocken, PA, USA, 2005.
80. ASTM C348-21; Standard Test Method for Flexural Strength of Hydraulic-Cement Mortars. ASTM International: West Conshohocken, PA, USA, 2021.
81. ASTM Standard C1760; Standard Test Method for Bulk Electrical Conductivity of Hardened Concrete. ASTM International: West Conshohocken, PA, USA, 2012.
82. ASTM-C642 ASTM C642-13; Standard Test Method for Density, Absorption, and Voids in Hardened Concrete. ASTM International: West Conshohocken, PA, USA, 2013.
83. NT Build 492. In *Concrete, Mortar and Cement-Based Repair Materials: Chloride Migration Coefficient from Non-Steady-State Migration Experiments*; Measurement; Nordtest Method; Nordic Cooperation: Copenhagen, Denmark, 1999; Volume 492.
84. Zadeh, L.A. Fuzzy Sets. *Inf. Control* **1965**, *8*, 338–353. [[CrossRef](#)]
85. Akkurt, S.; Tayfur, G.; Can, S. Fuzzy Logic Model for the Prediction of Cement Compressive Strength. *Cem. Concr. Res.* **2004**, *34*, 1429–1433. [[CrossRef](#)]
86. Amin, M.; Elsakhawy, Y.; Abu el-hassan, K.; Abdelsalam, B.A. Behavior Evaluation of Sustainable High Strength Geopolymer Concrete Based on Fly Ash, Metakaolin, and Slag. *Case Stud. Constr. Mater.* **2022**, *16*, e00976. [[CrossRef](#)]
87. Małek, M.; Łasica, W.; Kadela, M.; Kluczyński, J.; Dudek, D. Physical and Mechanical Properties of Polypropylene Fibre-Reinforced Cement–Glass Composite. *Materials* **2021**, *14*, 637. [[CrossRef](#)]
88. Sharma, U.; Gupta, N.; Bahrami, A.; Özkılıç, Y.O.; Verma, M.; Berwal, P.; Althaqafi, E.; Khan, M.A.; Islam, S. Behavior of Fibers in Geopolymer Concrete: A Comprehensive Review. *Buildings* **2024**, *14*, 136. [[CrossRef](#)]
89. Li, L.; Sun, H.X.; Zhang, Y.; Yu, B. Surface Cracking and Fractal Characteristics of Bending Fractured Polypropylene Fiber-reinforced Geopolymer Mortar. *Fractal Fract.* **2021**, *5*, 142. [[CrossRef](#)]
90. Waqas, R.M.; Zaman, S.; Alkharisi, M.K.; Butt, F.; Alsuhaibani, E. Influence of Bentonite and Polypropylene Fibers on Geopolymer Concrete. *Sustainability* **2024**, *16*, 789. [[CrossRef](#)]
91. Işıkdag, B.; Yalghuz, M.R. Strength Development and Durability of Metakaolin Geopolymer Mortars Containing Pozzolans under Different Curing Conditions. *Minerals* **2023**, *13*, 857. [[CrossRef](#)]
92. Hassan, A.; Arif, M.; Shariq, M. Influence of Microstructure of Geopolymer Concrete on Its Mechanical Properties—A Review. In *Lecture Notes in Civil Engineering*; Springer: Berlin/Heidelberg, Germany, 2020; Volume 35.
93. Ahmad, J.; Majdi, A.; Arbili, M.M.; Deifalla, A.F.; Naqash, M.T. Mechanical, Durability and Microstructure Analysis Overview of Concrete Made with Metakaolin (MTK). *Buildings* **2022**, *12*, 1401. [[CrossRef](#)]
94. Rashad, A.M. A Comprehensive Overview about the Influence of Different Additives on the Properties of Alkali-Activated Slag—A Guide for Civil Engineer. *Constr. Build. Mater.* **2013**, *47*, 29–55. [[CrossRef](#)]
95. Umniati, B.S.; Risdanareni, P.; Zein, F.T.Z. Workability Enhancement of Geopolymer Concrete through the Use of Retarder. In Proceedings of the AIP Conference, Provo, UT, USA, 16–21 July 2017; Volume 1887.
96. Nath, P.; Sarker, P.K. Use of OPC to Improve Setting and Early Strength Properties of Low Calcium Fly Ash Geopolymer Concrete Cured at Room Temperature. *Cem. Concr. Compos.* **2015**, *55*, 205–214. [[CrossRef](#)]
97. Memon, F.A.; Nuruddin, M.F.; Demie, S.; Shafiq, N. Effect of Curing Conditions on Strength of Fly Ash-Based Self-Compacting Geopolymer Concrete. *World Acad. Sci. Eng. Technol.* **2011**, *5*, 3–29.

98. Silva, S.; Kithalawa Arachchi, J.; Wijewardena, C.; Nanayakkara, S. Development of Fly Ash Based Geopolymer Concrete. In Proceedings of the Annual Session, Honolulu, HI, USA, 4–8 May 2012.
99. Chindaprasirt, P.; Chareerat, T.; Sirivivatnanon, V. Workability and Strength of Coarse High Calcium Fly Ash Geopolymer. *Cem. Concr. Compos.* **2007**, *29*, 224–229. [[CrossRef](#)]
100. Temuujin, J.; van Riessen, A.; Williams, R. Influence of Calcium Compounds on the Mechanical Properties of Fly Ash Geopolymer Pastes. *J. Hazard. Mater.* **2009**, *167*, 82–88. [[CrossRef](#)]
101. Krishnan, L.; Karthikeyan, S.; Nathiya, S.; Suganya, K. Geopolymer Concrete an Eco-Friendly Construction Material. *Magnesium* **2014**, *1*.
102. Cheah, C.B.; Samsudin, M.H.; Ramli, M.; Part, W.K.; Tan, L.E. The Use of High Calcium Wood Ash in the Preparation of Ground Granulated Blast Furnace Slag and Pulverized Fly Ash Geopolymers: A Complete Microstructural and Mechanical Characterization. *J. Clean. Prod.* **2017**, *156*, 114–123. [[CrossRef](#)]
103. Deb, P.S.; Nath, P.; Sarker, P.K. The Effects of Ground Granulated Blast-Furnace Slag Blending with Fly Ash and Activator Content on the Workability and Strength Properties of Geopolymer Concrete Cured at Ambient Temperature. *Mater. Des.* **2014**, *62*, 32–39. [[CrossRef](#)]
104. Nath, P.; Sarker, P.K.; Rangan, V.B. Early Age Properties of Low-Calcium Fly Ash Geopolymer Concrete Suitable for Ambient Curing. In Proceedings of the Procedia Engineering, Surabaya, Indonesia, 15–18 September 2015; Volume 125.
105. Islam, A.; Alengaram, U.J.; Jumaat, M.Z.; Bashar, I.I. The Development of Compressive Strength of Ground Granulated Blast Furnace Slag-Palm Oil Fuel Ash-Fly Ash Based Geopolymer Mortar. *Mater. Des.* **2014**, *56*, 833–841. [[CrossRef](#)]
106. Kazemian, F.; Hassani, A. Exploring Mechanical and Fracture Properties in Geopolymer Concrete with Ternary Precursor Waste Materials through Laboratory Investigations and Statistical Analysis. *J. Build. Eng.* **2024**, *95*, 110294. [[CrossRef](#)]
107. KR, P.R. Effects of Multiple Precursors on Strength, Durability, and Microstructural Properties of Ambiently Cured Geopolymer Concrete. *Constr. Build. Mater.* **2024**, *442*, 137538. [[CrossRef](#)]
108. Pradhan, J.; Panda, S.; Dwibedy, S.; Pradhan, P.; Panigrahi, S.K. Production of Durable High-Strength Self-Compacting Geopolymer Concrete with GGBFS as a Precursor. *J. Mater. Cycles Waste Manag.* **2024**, *26*, 529–551. [[CrossRef](#)]
109. Hamdi, O.M.; Ahmed-Chaouch, A.; Saïdani, M.; Alioui, H. Use of the Algerian Natural Pozzolan for the Production of a Geopolymer as a Complete Cement Replacement. *Constr. Build. Mater.* **2023**, *400*, 132723. [[CrossRef](#)]
110. Zhang, H.; Kumar Sarker, P.; Wang, Q.; He, B.; Chandra Kuri, J.; Jiang, Z. Comparison of Compressive, Flexural, and Temperature-Induced Ductility Behaviours of Steel-PVA Hybrid Fibre Reinforced OPC and Geopolymer Concretes after High Temperatures Exposure. *Constr. Build. Mater.* **2023**, *399*, 132560. [[CrossRef](#)]
111. Yang, Z.; Lu, F.; Zhan, X.; Zhu, H.; Zhang, B.; Chen, Z.; Zhang, H. Mechanical Properties and Mesoscopic Damage Characteristics of Basalt Fibre-Reinforced Seawater Sea-Sand Slag-Based Geopolymer Concrete. *J. Build. Eng.* **2024**, *84*, 108688. [[CrossRef](#)]
112. Zheng, J.; Qi, L.; Zheng, Y.; Zheng, L. Mechanical Properties and Compressive Constitutive Model of Steel Fiber-Reinforced Geopolymer Concrete. *J. Build. Eng.* **2023**, *80*, 108161. [[CrossRef](#)]

Disclaimer/Publisher’s Note: The statements, opinions and data contained in all publications are solely those of the individual author(s) and contributor(s) and not of MDPI and/or the editor(s). MDPI and/or the editor(s) disclaim responsibility for any injury to people or property resulting from any ideas, methods, instructions or products referred to in the content.